

Embedding-Projection Correspondences for the estimation of the Gromov-Hausdorff distance

Facundo Mémoli and Zane Smith






Working paper
Version 1
July 4, 2024

Abstract



This writeup describes ongoing work on designing and testing a certain family of correspondences between compact metric spaces that we call *embedding-projection correspondences* (EPCs). Of particular interest are EPCs between spheres of different dimension.

Contents

1	Introduction	2
1.1	Acknowledgements	3
2	Background	3
3	The general construction of EPCs	5
3.1	Interpretation of EPCs	6
3.2	Voronoi cells and modulus of discontinuity of ψ_ι	6
4	EPC constructions for the case of spheres	7
4.1	Constructions for the case of \mathbb{S}^1 versus \mathbb{S}^n	7
4.2	Cartoonizations and other constructions 	9
4.2.1	Examples of cartoonizations 	9
4.2.2	Another construction for the case of \mathbb{S}^1 versus \mathbb{S}^2	9
4.2.3	A construction for the case of \mathbb{S}^2 versus \mathbb{S}^3	10
4.2.4	EPCs for the case of \mathbb{S}^m versus \mathbb{S}^n	10
5	General results about TMC-EPCs	10
5.1	Some results about the fibers of R_{2k+1}	10
5.2	A simplification of the calculation of the distortion of R_{2k+1}	12
5.3	Other results	14

5.3.1	Hopf coordinates on \mathbb{S}^{2k+1}	14
5.3.2	Some properties of γ_{2k+1} and the TMC-EPC	16
6	The case of \mathbb{S}^1 versus \mathbb{S}^3	19
6.1	Characterization of the fiber $F_3(0)$	20
6.2	The modulus of discontinuity of ψ_3 is minimal	24
6.3	The distortion of R_3 is minimal 	25
7	The case \mathbb{S}^1 versus \mathbb{S}^{2k+1}	26
7.1	Connections to the Barvinok-Novik polytope	26
7.2	An application to Conjecture 5 	27
7.3	Connecting structure of \mathcal{B}_{2k} to Voronoi tiling induced by γ_{2k+1}	29
7.4	The modulus of discontinuity of ψ_{2k+1} is minimal	30
7.5	Additional results stemming from Proposition 7.2 	30
8	Results for the case \mathbb{S}^m versus \mathbb{S}^n 	30
9	Historical account and connections 	30

1 Introduction

This work is evolving. It might contain an incomplete account in some places. We will be updating this document frequently. The tag  indicates that an upcoming update is planned in the corresponding part of the text. To indicate that accompanying code exists to demonstrate a construction/idea we will use the symbol .

The central question we explore is:

Question 1 ([LMS23]). *What is the precise value of the Gromov-Hausdorff distance $d_{\text{GH}}(\mathbb{S}^m, \mathbb{S}^n)$ between spheres of different dimensions (endowed with their geodesic distance)?*

Several results have been obtained which provide partial answers to Question 1:

- In [LMS23] Lim, Mémoli and Smith obtain the precise value of $d_{\text{GH}}(\mathbb{S}^1, \mathbb{S}^2)$, $d_{\text{GH}}(\mathbb{S}^2, \mathbb{S}^3)$ and $d_{\text{GH}}(\mathbb{S}^1, \mathbb{S}^3)$. They also provide a lower bound for $d_{\text{GH}}(\mathbb{S}^m, \mathbb{S}^n)$ for all spheres which is based on a version of the Borsuk-Ulam theorem due to Dubins and Schwarz [DS81]. These lower bounds arise as obstructions for odd functions from $\mathbb{S}^n \rightarrow \mathbb{S}^m$ to be continuous, when $n > m$.
- The currently best known lower bound for $d_{\text{GH}}(\mathbb{S}^m, \mathbb{S}^n)$ was found in [ABC⁺22] via ideas which combine insights from [LMS23] and [ABF20] in a way that generalizes the version of the Borsuk-Ulam theorem due to Dubins and Schwarz.
- In [HJ23] Jeffs and Harrison obtain the precise value of $g_{m,n} := d_{\text{GH}}(\mathbb{S}^1, \mathbb{S}^{2k})$ for all integers $k \geq 1$.

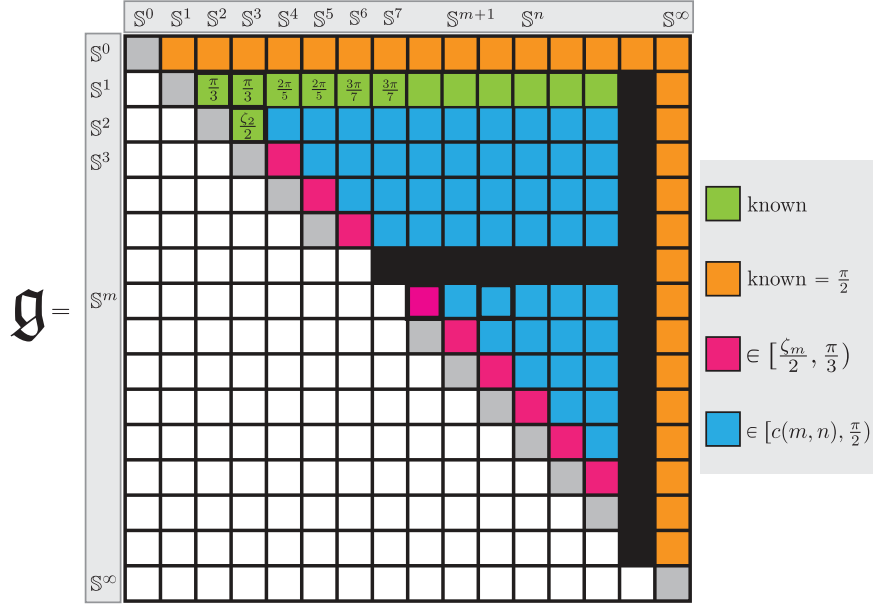


Figure 1: Current knowledge (as of July 4, 2024) about the value of $g_{m,n}$ for $0 \leq m, n \leq \infty$. See Section 1.

- In an upcoming update to [HJ23], Jeffs and Harrison also obtain the precise value of $d_{\text{GH}}(\mathbb{S}^1, \mathbb{S}^{2k+1})$ for all integers $k \geq 1$.

This writeup describes and develops several yet unpublished ideas that led to some of the results in our paper [LMS23]. A historical account is given in Section 9. Figure 1 describes the current knowledge about the different values of $g_{m,n}$.

1.1 Acknowledgements

We thank Henry Adams for suggesting to us exploring the connection between our ideas and the TMC and the Barvinok-Novik polytope. That fruitful suggestion led to the general description of R_{γ_n} that we are exploring in this project and to some of the results that we described. We also thank Sunhyuk Lim for careful reading of the first version and for his feedback.

This work is supported by NSF-2310412, NSF-1547357, NSF-1740761, NSF-1901360 and by BSF 2020124.

2 Background

Given two sets X and Y , a correspondence between them is any relation $R \subseteq X \times Y$ such that $\pi_X(R) = X$ and $\pi_Y(R) = Y$ where $\pi_X : X \times Y \rightarrow X$ and $\pi_Y : X \times Y \rightarrow Y$ are the canonical projections. Given two bounded metric spaces (X, d_X) and (Y, d_Y) , and any non-empty relation $R \subseteq X \times Y$, its *distortion* is defined as

$$\text{dis}(R) := \sup_{(x,y),(x',y') \in R} |d_X(x, x') - d_Y(y, y')|.$$

Remark 2.1. Note that for any two nested non-empty relations $S \subset R$ between X and Y one has $\text{dis}(S) \leq \text{dis}(R)$.

For a function $\varphi : X \rightarrow Y$, its distortion, $\text{dis}(\varphi)$ is just the distortion of its graph: $\text{dis}(\varphi) := \text{dis}(\text{graph}(\varphi))$.

Definition 1. The Gromov-Hausdorff distance between any two bounded metric spaces (X, d_X) and (Y, d_Y) is defined as

$$d_{\text{GH}}(X, Y) := \frac{1}{2} \inf_R \text{dis}(R), \quad (1)$$

where R ranges over all correspondences between X and Y .

Given a correspondence R between X and Y , we say that a function $\psi : Y \rightarrow X$ is *subordinate* to R whenever its graph is contained in the correspondence:

$$\text{graph}(\psi) := \{(\psi(y), y) | y \in Y\} \subset R.$$

In general, given a function $\psi : Y \rightarrow X$ its graph may fail to yield a correspondence between X and Y . However, this of course is guaranteed whenever ψ is surjective.

Definition 2 (Modulus of discontinuity, [DS81]). Let Y be a topological space, X be a metric space, and $f : Y \rightarrow X$ be any function. Then, we define $\text{disc}(f)$, the *modulus of discontinuity of f* as follows:

$$\text{disc}(f) := \inf\{\delta \geq 0 : \forall y \in Y, \exists \text{ an open neighborhood } U_y \text{ of } y \text{ s.t. } \text{diam}(f(U_y)) \leq \delta\}.$$

Here, for a non-empty subset A of X , its *diameter* is defined as $\text{diam}(A) := \sup_{a, a' \in A} d_X(a, a')$.

Remark 2.2. Of course, $\text{disc}(f) = 0$ if and only if f is continuous.

The modulus of discontinuity of a function is controlled by its distortion.

Proposition 2.1 ([LMS23, Proposition 5.3]). Let R be any correspondence between the metric spaces X and Y and let $\psi : Y \rightarrow X$ be any subordinate function. Then,

$$\text{disc}(\psi) \leq \text{dis}(\psi) \leq \text{dis}(R).$$

From now on, by \mathcal{M} we will denote the collection of all compact metric spaces.

Theorem 1 ([ABC⁺22, Main Theorem and Theorem 5.1]). For all integers $k \geq 1$ and for any correspondence R between \mathbb{S}^1 and \mathbb{S}^{2k+1} one has $\text{dis}(R) \geq \delta_k$ where

$$\delta_k := \frac{2\pi k}{2k+1}.$$

Similarly, $\text{dis}(R) \geq \delta_k$ for any correspondence between \mathbb{S}^1 and \mathbb{S}^{2k} .

Remark 2.3. *Note that:*

- the parameter δ_k above coincides with the edge length (in the geodesic sense) of an odd regular polygon inscribed in the unit circle \mathbb{S}^1 . For example, $\delta_1 = \frac{2\pi}{3}$, which corresponds to the distance between vertices of an equilateral triangle inscribed in the unit circle.
- the theorem of course implies that $d_{\text{GH}}(\mathbb{S}^1, \mathbb{S}^{2k})$ and $d_{\text{GH}}(\mathbb{S}^1, \mathbb{S}^{2k+1})$ are both bounded below by $\frac{\delta_k}{2}$.

Theorem 1 above is intimately related to the following complementary theorem. Recall that, for integers $n \geq m$, a function $f : \mathbb{S}^n \rightarrow \mathbb{S}^m$ is said to be antipode preserving (or just antipodal), if $f(-x) = -f(x)$ for all $x \in \mathbb{S}^n$.

Theorem 2 ([ABC⁺22, Theorems 1.3 and 5.1]). *Let $f : \mathbb{S}^{2k+1} \rightarrow \mathbb{S}^1$ be any antipodal function. Then $\text{disc}(f) \geq \delta_k$. Similarly, $\text{disc}(f) \geq \delta_k$ for any antipodal function $f : \mathbb{S}^{2k} \rightarrow \mathbb{S}^1$.*

The relationship between Theorem 1 and Theorem 2 is explained in [ABC⁺22, Remark 7.3]; see also [LMS23, Section 5].

3 The general construction of EPCs

Let $X, Y \in \mathcal{M}$ be two compact metric spaces such that there exists an embedding $\iota : X \rightarrow Y$ of X into Y (i.e. a homeomorphism onto its image). Importantly, *one does not require the embedding to be isometric*. Consider then any *closest point projection function* $\Pi_\iota : Y \rightarrow \iota(X)$: that is, Π_ι satisfies that for any $y \in Y$, $\Pi_\iota(y)$ is such that

$$\rho_{\Pi_\iota}(y) := d_Y(y, \Pi_\iota(y)) = \min_{y' \in \iota(X)} d_Y(y, y').$$

Since $\iota(X) \subset Y$, any such function Π_ι is always surjective but it might not be injective.

Definition 3. The *embedding-projection correspondence* induced by ι is the correspondence $R_\iota \in \mathcal{R}(X, Y)$ defined as:

$$R_\iota := \{(x, y) \in X \times Y \mid \iota(x) = \Pi_\iota(y)\}.$$

By $\psi_\iota : Y \rightarrow X$ we will denote the function $Y \ni y \mapsto \psi_\iota(y) := \iota^{-1}(\Pi_\iota(y))$. See Figure 2.

We will use the acronym EPC to denote correspondences of the form described in the definition above and, similarly, we will use the acronym EPS to denote the associated surjections.

Remark 3.1. *Note that the function ψ_ι constructed above is subordinate to R_ι and that, furthermore, $R_\iota = \text{graph}(\psi_\iota)$ and therefore $\text{dis}(R_\iota) = \text{dis}(\psi_\iota)$.*

The main motivation behind this definition is to carefully design the embedding ι so that the distortion of R_ι is as small as possible. It is not necessarily the case that an isometric embedding $\iota : X \hookrightarrow Y$ will give rise to a low distortion correspondence. Consider for example the case of any equatorial embedding $\iota : \mathbb{S}^1 \hookrightarrow \mathbb{S}^2$. In that case, it is immediate to check that $\text{dis}(R_\iota) = \pi$ which is far from the minimal possible distortion which is known to be $\frac{2\pi}{3}$ [LMS23, Proposition 1.16]. In fact, results in the the same reference prove that this naive equatorial embedding fails to give good upper bounds in general.

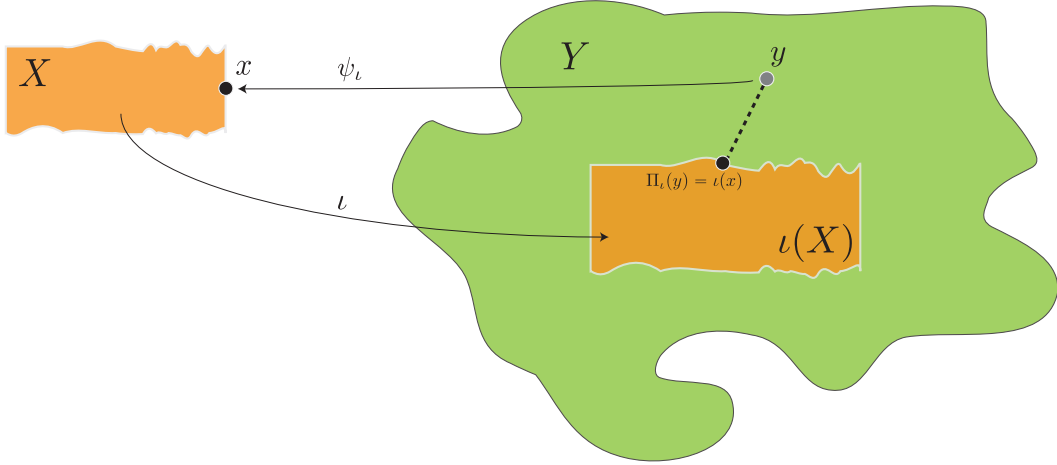


Figure 2: An embedding-projection correspondence. See Definition 3.

3.1 Interpretation of EPCs

For an EPC R_ι to be “good” in the sense of having small distortion, it is necessary that both $\iota : X \rightarrow Y$ does not distort distances too much and that $\iota(X)$ provides an efficient covering of Y .

Proposition 3.1. *For any EPC R_ι , one has*

$$\text{dis}(R_\iota) \geq \max(\text{dis}(\iota), \rho(\Pi_\iota)),$$

where $\rho(\Pi_\iota) := \sup_{y \in Y} \rho_{\Pi_\iota}(y)$ is the covering radius of the projection function Π_ι .

Proof. That $\text{dis}(R_\iota) \geq \text{dis}(\iota)$ is clear since $\psi_\iota|_{\iota(X)} = \text{id}_X$ and therefore

$$\text{dis}(R_\iota) = \text{dis}(\psi_\iota) \geq \text{dis}(\psi_\iota|_{\iota(X)}) = \sup_{x, x' \in X} |d_X(x, x') - d_Y(\iota(x), \iota(x'))| = \text{dis}(\iota).$$

To obtain $\text{dis}(R_\iota) \geq \rho(\Pi_\iota)$ notice that for any $y \in Y$, $\psi_\iota(y) = \psi_\iota(\Pi_\iota(y))$ so that

$$\rho(\Pi_\iota) = \sup_{y \in Y} |d_X(\psi_\iota(y), \psi_\iota(\Pi_\iota(y))) - d_Y(y, \Pi_\iota(y))| \leq \text{dis}(R).$$

□

3.2 Voronoi cells and modulus of discontinuity of ψ_ι

For each $x \in X$ consider the x -fiber of ψ_ι :

$$V_x := \{y \in Y \mid \Pi_\iota(y) = \iota(x)\} = \{y \in Y \mid \psi_\iota(y) = x\}.$$

In other words, $\overline{V_x}$ is the Voronoi cell induced by $\iota(x) \in \iota(X)$ on Y . Then, we have the following immediate consequence of this definition and the definition of modulus of discontinuity (Definition 2).

Proposition 3.2. $\text{disc}(\psi_\iota) = \sup\{d_X(x, x') \mid V_x \cap V_{x'} \neq \emptyset\}$.

4 EPC constructions for the case of spheres

We now describe a number of constructions of EPCs between spheres that we have tested exhaustively via computational methods. As we discuss below, our extensive experimental evidence indicates that these constructions are optimal [MS23].

In what follows, for each $n \in \mathbb{N}$, we view the unit sphere $\mathbb{S}^n \subset \mathbb{R}^{n+1}$, when endowed with its geodesic distance d_n , as the compact metric space (\mathbb{S}^n, d_n) . Explicitly,

$$d_n(x, x') = \arccos(x \cdot x').$$

The constructions we mention below are related to the general question of determining the precise value of $d_{\text{GH}}(\mathbb{S}^m, \mathbb{S}^n)$ for all $m < n$ which was considered in [LMS23].

In what follows we will assume the *equatorial* (isometric embedding $\iota_{2k} : \mathbb{S}^{2k} \hookrightarrow \mathbb{S}^{2k+1}$ arising from the embedding of $\mathbb{R}^{2k+1} \hookrightarrow \mathbb{R}^{2k+2}$ where

$$x = (x_1, x_2, \dots, x_{2k+1}) \mapsto (x_1, x_2, \dots, x_{2k+1}, 0).$$

These embeddings, through suitable compositions, induce embeddings $\iota_{m,n} : \mathbb{S}^m \hookrightarrow \mathbb{S}^n$, for all $n \geq m$. We will henceforth identify \mathbb{S}^m with its image in \mathbb{S}^n via $\iota_{m,n}$. Similarly, we consider the surjective projection maps $p_{2k+1} : \mathbb{S}^{2k+1} \setminus \{\pm e_{2k+2}\} \rightarrow \mathbb{S}^{2k}$ given by

$$(x_1, x_2, \dots, x_{2k+1}, x_{2k+2}) \mapsto \frac{(x_1, x_2, \dots, x_{2k+1}, 0)}{\sqrt{x_1^2 + x_2^2 + \dots + x_{2k+1}^2}}.$$

4.1 Constructions for the case of \mathbb{S}^1 versus \mathbb{S}^n

Definition 4. Let n be any positive integer. The (projected centrally symmetric) *trigonometric moment curve* (TMC) of order n is defined as follows.¹

When $n = 2k + 1$ for some $k \geq 1$, $\gamma_{2k+1} : \mathbb{S}^1 \rightarrow \mathbb{S}^{2k+1}$ is given by

$$t \mapsto \frac{1}{\sqrt{k+1}} (\cos(t), \sin(t), \cos(3t), \sin(3t), \dots, \cos((2k+1)t), \sin((2k+1)t)).$$

When $n = 2k$ for some $k \geq 1$, $\gamma_{2k} : \mathbb{S}^1 \mapsto \mathbb{S}^{2k}$ is given by

$$t \mapsto \frac{1}{\sqrt{k + \cos^2((2k+1)t)}} (\cos(t), \sin(t), \cos(3t), \sin(3t), \dots, \cos((2k+1)t)).$$

Note that γ_n provides an embedding of \mathbb{S}^1 into \mathbb{S}^n which we will henceforth refer to as a *TMC embedding*. Note that R_{γ_n} is a correspondence between \mathbb{S}^1 and \mathbb{S}^n and that ψ_{γ_n} is surjection from \mathbb{S}^n to \mathbb{S}^1 . We will refer to these correspondences as TMC-EPCs. To simplify notation, we will henceforth use the notation R_n instead of R_{γ_n} , Π_n instead of Π_{γ_n} and similarly, ψ_n instead of ψ_{γ_n} . See Figure 3 for an illustration.

¹For odd n this definition coincides, up to a multiplicative constant, with the symmetric trigonometric moment curve considered in [BN08].

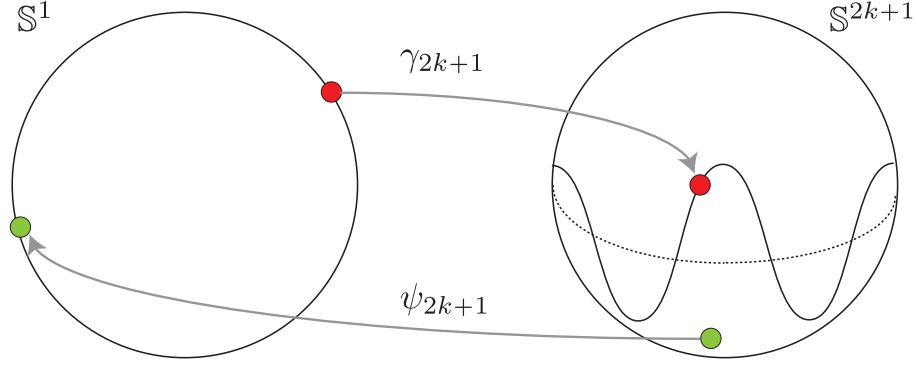


Figure 3: The maps $\gamma_{2k+1} : \mathbb{S}^1 \rightarrow \mathbb{S}^{2k+1}$ and $\psi_{2k+1} : \mathbb{S}^{2k+1} \rightarrow \mathbb{S}^1$.

Remark 4.1. *The following properties of the TMCs γ_n and of the maps ψ_n follow from their definitions:*

1. $\gamma_n : \mathbb{S}^1 \rightarrow \mathbb{S}^n$ is antipodal.
2. $p_{2k+1}(\gamma_{2k+1}) = \gamma_{2k}$.
3. The map $\psi_n : \mathbb{S}^n \rightarrow \mathbb{S}^1$ is antipodal (this follows from item 1).
4. $R_n = \text{graph}(\psi_n)$ (see Remark 3.1).

Theorem 1 above implies that both $\text{dis}(R_{2k})$ and $\text{dis}(R_{2k+1})$ must be at least δ_k . Our extensive computational experimentation strongly suggests that R_{2k} and R_{2k+1} are optimal.

Conjecture 1. $\text{dis}(R_{2k+1}) = \text{dis}(R_{2k}) = \frac{2\pi k}{2k+1}$ for all $k \in \mathbb{N}$.

Similarly, Theorem 2 implies that $\text{disc}(\psi_{2k+1})$ and $\text{disc}(\psi_{2k})$ are both bounded below by δ_k which motivates the following.

Conjecture 2. $\text{disc}(\psi_{2k+1}) = \text{disc}(\psi_{2k}) = \delta_k$.

Remark 4.2. *We point out that Conjecture 1, if true, would imply Conjecture 2. Indeed, suppose for example that $\text{dis}(R_{2k+1}) = \delta_k$. Then, Proposition 2.1 together with the fact that ψ_{2k+1} is subordinate to R_{2k+1} , would imply that $\delta_k \geq \text{disc}(\psi_{2k+1})$. Then, the equality $\text{disc}(\psi_{2k+1}) = \delta_k$ would follow from Remark 4.1 and Theorem 2.*

We nevertheless pose both conjectures having in mind that it might be easier to arrive at the former than the latter. See Section 6.2 and Section 6.3.

We first point out that it would be enough to establish Conjecture 1 and Conjecture 2 above only for R_{2k+1} (respectively, ψ_{2k+1}) since we have the following.

Proposition 4.1. *It holds that $\text{dis}(R_{2k+1}) \geq \text{dis}(R_{2k})$ and $\text{disc}(\psi_{2k+1}) \geq \text{disc}(\psi_{2k})$.*

Proof. These follow from the fact that $\psi_{2k+1}|_{\mathbb{S}^{2k}} = \psi_{2k}$ where the precise copy of $\mathbb{S}^{2k} \subset \mathbb{S}^{2k+1}$ we mean is the equatorial one, as mentioned at the beginning of this section. \square

Remark 4.3 (☒). *We have run extensive experimentation in relation to Conjecture 1 for the values of $k = 1, 2, 3, 4$. See our GitHub repository [MS23, Function `TestDistortionRn.m`]. Our results strongly suggest that R_{2k} and R_{2k+1} are optimal correspondences (for the corresponding values of k).*

Example 4.1. For example, Conjecture 1, if true would imply that:

- the distortion of the EPC between \mathbb{S}^1 and \mathbb{S}^2 induced by the curve

$$\gamma_2(t) = \frac{1}{\sqrt{1 + \cos^2(3t)}} (\cos(t), \sin(t), \cos(3t))$$

is $\frac{2\pi}{3}$.

- the distortion of the EPC between \mathbb{S}^1 and \mathbb{S}^3 induced by the curve

$$\gamma_3(t) = \frac{1}{\sqrt{2}} (\cos(t), \sin(t), \cos(3t), \sin(3t))$$

is also $\frac{2\pi}{3}$.

4.2 Cartoonizations and other constructions 📌

During our work, we used the term *cartoonization* to refer to the process of simplification of the TMC-ECPs. Some of the ideas behind this loosely defined concept involved discretizing R_n or altering the nature of the curve by for example substituting it for a piece-wise geodesic path. For example, the optimal correspondence between \mathbb{S}^1 and \mathbb{S}^2 described in [LMS21, Appendix D] arose as a cartoonization of R_2 . Similarly, the optimal correspondence constructed in [LMS23, Proposition 1.16] can be regarded as a cartoonization of R_2 .

4.2.1 Examples of cartoonizations 📌

4.2.2 Another construction for the case of \mathbb{S}^1 versus \mathbb{S}^2

Consider the following curve/embedding of \mathbb{S}^1 into \mathbb{S}^2 . Let $\alpha : \mathbb{S}^1 \rightarrow \mathbb{S}^2$ be given by

$$t \mapsto (\cos(t)\sqrt{1 - z^2(t)}, \sin(t)\sqrt{1 - z^2(t)}, z(t))$$

where $z(t) := 0.15 \cos(3t)$.

Remark 4.4 (☒). *This correspondence emerged as a variant of R_2 . Through our computational experiments we arrive the the following.*

Conjecture 3. $\text{dis}(R_\alpha) = \frac{2\pi}{3}$.

4.2.3 A construction for the case of \mathbb{S}^2 versus \mathbb{S}^3

As a generalization of the construction in Section 4.2.2, we construct a *surface* $\sigma : \mathbb{S}^2 \rightarrow \mathbb{S}^3$. We describe σ in spherical coordinates on \mathbb{S}^2 : $x, y, z : [0, 2\pi) \times [0, \pi] \rightarrow \mathbb{S}^2$ where $(x(\phi, \theta), y(\phi, \theta), z(\phi, \theta)) := (\cos(\phi) \sin(\theta), \sin(\phi) \sin(\theta), \cos(\theta))$. Let

$$w(\phi, \theta) := \frac{1}{3} \sin(\theta) \sin(2\theta) \cos(2\phi).$$

This function is proportional to the (real) spherical harmonic $Y_{3,2}$ which has tetrahedral symmetry in the sense that its maximum value (as a function on the sphere \mathbb{S}^2) is attained at the vertices of a regular tetrahedron inscribed in the sphere. Then, define

$$\sigma(\phi, \theta) := \left(x(\phi, \theta) \sqrt{1 - w^2(\phi, \theta)}, y(\phi, \theta) \sqrt{1 - w^2(\phi, \theta)}, z(\phi, \theta) \sqrt{1 - w^2(\phi, \theta)}, w(\phi, \theta) \right).$$

Remark 4.5 (\square). *The resulting correspondence R_σ was extensively experimentally tested and it was cartoonized in the proof of [LMS23, Proposition 1.19]. Theorem B in [LMS23] implies that $\text{dis}(R_\sigma) \geq \zeta_2 := \arccos(-\frac{1}{3})$.*

Conjecture 4. $\text{dis}(R_\sigma) = \zeta_2$.

4.2.4 EPCs for the case of \mathbb{S}^m versus \mathbb{S}^n \bullet

5 General results about TMC-EPCs

We establish several general results about the fibers of TMC-EPCs.

5.1 Some results about the fibers of R_{2k+1}

For each $t \in \mathbb{S}^1$, by $F_{2k+1}(t)$ we will denote the closed fiber

$$\begin{aligned} F_{2k+1}(t) &:= \overline{\{x \in \mathbb{S}^{2k+1} \mid (x, t) \in R_{2k+1}\}} \\ &= \{x \in \mathbb{S}^{2k+1} \mid d_{2k+1}(x, \gamma_{2k+1}(t)) \leq d_{2k+1}(x, \gamma_{2k+1}(s)) \forall s \in \mathbb{S}^1\} \\ &= \{x \in \mathbb{S}^{2k+1} \mid x \cdot \gamma_{2k+1}(t) \geq x \cdot \gamma_{2k+1}(s) \forall s \in \mathbb{S}^1\}. \end{aligned}$$

We will henceforth identify \mathbb{S}^1 with the real line modulo the equivalence relation $t \sim s$ iff $t - s = 2\pi m$ for some integer m . It will be useful to introduce the following family of rotations of \mathbb{R}^{2k+2} . For $t \in \mathbb{S}^2$, let

$$T_t := \begin{bmatrix} M_1(t) & 0 & 0 & 0 & \cdots & 0 \\ 0 & M_3(t) & 0 & 0 & \cdots & 0 \\ 0 & 0 & M_5(t) & 0 & \cdots & 0 \\ 0 & 0 & 0 & M_7(t) & \cdots & 0 \\ \vdots & \vdots & \vdots & \vdots & \ddots & \vdots \\ 0 & 0 & 0 & 0 & \cdots & M_{2k+1}(t) \end{bmatrix}$$

where, for each non-negative integer ℓ

$$M_{2\ell+1}(t) := \begin{bmatrix} \cos((2\ell+1)t) & \sin((2\ell+1)t) \\ -\sin((2\ell+1)t) & \cos((2\ell+1)t) \end{bmatrix}.$$

These rotations have been utilized in the context of studying cyclic polytopes induced by the TMC; see [Smi90, Section 2] for the case $k = 1$ and [BN08, Section 3] for the general case.

Remark 5.1. *Note that $T_0 = \text{id}$, $T_{\pm\pi} = -\text{id}$ and that for all t and s one has*

$$\gamma_{2k+1}(t+s) = T_t(\gamma_{2k+1}(s)).$$

It follows that, since the fibers $F_{2k+1}(t)$ are defined via a closest point map, we have that all fibers are isometric and satisfy

$$F_{2k+1}(t) = T_t(F_{2k+1}(0)).$$

Recall that a closed subset A of \mathbb{S}^n is said to be *geodesically convex* if for any two points $p, p' \in A$ there is a unique geodesic (minimizing) geodesic connecting p and p' that is entirely contained within A . Similarly, the *spherical convex hull* of A , denoted $\text{ConvSph}(A)$, is the union of all geodesic segments with endpoints in A . We will reserve the notation $\text{Conv}(A)$ to denote the standard convex hull of A .

Below, for $t \in \mathbb{S}^1$, by Σ_t we will denote the $(2k+1)$ -dimensional hyperplane passing through $\gamma_{2k+1}(t)$ and with normal $\dot{\gamma}_{2k+1}(t)$:

$$\Sigma_t := \{p \in \mathbb{R}^{2k+2} \mid (p - \gamma_{2k+1}(t)) \cdot \dot{\gamma}_{2k+1}(t) = 0\}$$

and by \mathbb{S}_t^{2k} we will denote the equator of \mathbb{S}^{2k+1} obtained as its intersection with Σ_t :

$$\mathbb{S}_t^{2k} := \mathbb{S}^{2k+1} \cap \Sigma_t.$$

Proposition 5.1. *The fiber $F_{2k+1}(0)$ is a geodesically convex subset of \mathbb{S}^{2k+1} . Furthermore, $F_{2k+1}(0) \subset \mathbb{S}_0^{2k}$.*

Remark 5.2. *Note that $F_{2k+1}(0) \cap \mathbb{S}^{2k-1} = F_{2k-1}(0)$.*

The proposition follows immediately from the lemma below and from results on Voronoi partitions induced by real algebraic manifolds [BKS24, Proposition 8.2]. Barvinok and Novik (in Section 1 of [BN08]) and Sinn already recognized that γ_{2k+1} is a smooth algebraic curve. This follows from the standard facts that

- for each integer m , $\cos(mt) = \mathcal{T}_m(\cos(t))$,
- for odd integers m , $\sin(mt) = -\mathcal{T}_m(\sin(t))$,

where \mathcal{T}_m is the m th Chebyshev polynomial (of the first kind). For example, for the case $k = 1$, (the trace of) γ_3 coincides with the zero set of the collection $\{P_1, P_2, P_3, P_4\}$ of polynomials given by²:

$$\begin{aligned} P_1(x, y, z, w) &:= x^2 + y^2 - \frac{1}{2} \\ P_2(x, y, z, w) &:= z^2 + w^2 - \frac{1}{2} \\ P_3(x, y, z, w) &:= z - \mathcal{T}_3(x) &= z - (4x^2 - 3)x \\ P_4(x, y, z, w) &:= w - \mathcal{T}_3(-y) &= w - (3 - 4y^2)y \end{aligned}$$

Lemma 5.1. *For each $k \geq 1$, the symmetric trigonometric moment curve $\gamma_{2k+1} : \mathbb{S}^1 \rightarrow \mathbb{S}^{2k+1}$ can be modeled as a smooth real algebraic curve.*

Proof of Proposition 5.1. The fiber $F_{2k+1}(0)$ is the intersection $V_{2k+1}(0) \cap \mathbb{S}^{2k+1}$ of the closed Voronoi cell $V_{2k+1}(0) \subset \mathbb{R}^{2k+2}$ corresponding to $\gamma_{2k+1}(0)$ in the Voronoi tiling of \mathbb{R}^{2k+2} induced by the curve γ_{2k+1} . By the lemma above, γ_{2k+1} is a smooth real algebraic curve so that, by [BKS24, Proposition 8.2], $V_{2k+1}(0)$ is convex. It is clear that $V_{2k+1}(0)$ is a convex cone containing the origin so that the claim follows from [FIN13, Proposition 2 and Remark 1].

The second claim that $F_{2k+1}(0)$ is contained in \mathbb{S}_0^{2k} can be explained as follows. One first recalls that

$$F_{2k+1}(0) = \{x \in \mathbb{S}^{2k+1} \mid x \cdot \gamma_{2k+1}(0) \geq x \cdot \gamma_{2k+1}(t) \ \forall t \in \mathbb{S}^1\}.$$

So that $x \in F_{2k+1}(0)$ then means that the function $t \mapsto f(t; x) := x \cdot \gamma_{2k+1}(t)$ has a global maximum at $t = 0$ which implies that $x \cdot \dot{\gamma}_{2k+1}(0) = 0$ whence the claim. \square

We now state the following relationship between the modulus of discontinuity of ψ_{2k+1} and the fibers $F_{2k+1}(\cdot)$ for later use. Via Proposition 3.2 and from the definition of $F_{2k+1}(0)$, we immediately obtain the following.

Corollary 5.1. $\text{disc}(\psi_{2k+1}) = \max\{t \in [0, \pi] \mid \partial F_{2k+1}(0) \cap \partial F_{2k+1}(t) \neq \emptyset\}.$

5.2 A simplification of the calculation of the distortion of R_{2k+1}

We exploit symmetries of R_{2k+1} in order to simplify the determination of its distortion.

Remark 5.3. *Note that, in order to estimate/calculate the distortion of R_{2k+1} , it suffices to consider, for all $q, q' \in F_{2k+1}(0)$ and $t \in \mathbb{S}^1$, the quantity*

$$\delta_t(q, q') := |d_{2k+1}(q, T_t(q')) - d_1(0, t)|.$$

In other words, one has

$$\text{dis}(R_{2k+1}) = \max_{\substack{q, q' \in F_{2k+1}(0) \\ t \in \mathbb{S}^1}} \delta_t(q, q').$$

²Note that this is not irreducible: P_2 can be dropped, for example

The claim follows from Remark 5.1 and the following calculation

$$\begin{aligned}
\text{dis}(R_{2k+1}) &= \max_{s,t \in \mathbb{S}^1} \max_{\substack{q \in F_{2k+1}(t) \\ q' \in F_{2k+1}(s)}} |d_{2k+1}(q, q') - d_1(s, t)| \\
&= \max_{q, q' \in F_{2k+1}(0)} \max_{s, t \in \mathbb{S}^1} |d_{2k+1}(T_t q, T_s q') - d_1(s, t)| \\
&= \max_{q, q' \in F_{2k+1}(0)} \max_{s, t \in \mathbb{S}^1} |d_{2k+1}(q, T_{s-t} q') - d_1(0, s - t)|.
\end{aligned}$$

For $\delta \in [0, \pi]$, consider the following four properties

$$\begin{aligned}
A'(\delta) : \quad & d_{2k+1}(q, T_t q') \leq d_1(0, t) + \delta & \forall q, q' \in F_{2k+1}(0), t \in \mathbb{S}^1 \\
A(\delta) : \quad & d_{2k+1}(q, T_t q') \leq d_1(0, t) + \delta & \forall q, q' \in F_{2k+1}(0), |t| \leq \pi - \delta \\
B'(\delta) : \quad & d_1(0, t) \leq d_{2k+1}(q, T_t q') + \delta & \forall q, q' \in F_{2k+1}(0), t \in \mathbb{S}^1 \\
B(\delta) : \quad & d_1(0, t) \leq d_{2k+1}(q, T_t q') + \delta & \forall q, q' \in F_{2k+1}(0), |t| \in [\delta, \pi]
\end{aligned}$$

The following proposition simplifies the task of checking whether $\text{dis}(R_{2k+1}) \leq \delta$ to checking whether $B(\delta)$ holds.

Proposition 5.2. *For each $\delta \in [0, \pi]$ we have:*

- (a) $\text{dis}(R_{2k+1}) \leq \delta \iff A'(\delta)$ and $B'(\delta)$ hold.
- (b) $A(\delta) \iff A'(\delta)$.
- (c) $B(\delta) \iff B'(\delta)$.
- (d) $B(\delta) \implies A(\delta)$.

Proof. (a) follows from Remark 5.3. (b), (c) are clear. Let's prove (d). Assume $B(\delta)$ holds so that, by (c), $B'(\delta)$ also holds. Pick t such that $|t| \leq \pi - \delta$ and fix $q, q' \in F_{2k+1}(0)$. WLOG we can assume that $t \in [0, \pi - \delta]$. Notice that, since $T_{t-\pi}(q') = T_{-\pi}T_t(q') = -T_t(q')$, we have

$$d_{2k+1}(q, T_t q') + d_{2k+1}(q, T_{t-\pi} q') = \pi.$$

Since $B'(\delta)$ holds, we have that $d_{2k+1}(q, T_{t-\pi} q') \geq d_1(0, t - \pi) - \delta$ so that

$$\begin{aligned}
d_{2k+1}(q, T_t q') &= \pi - d_{2k+1}(q, T_{t-\pi} q') \\
&\leq \pi + \delta - d_1(0, t - \pi) \\
&= \pi + \delta - (\pi - t) \\
&= t + \delta \\
&= d_1(0, t) + \pi
\end{aligned}$$

which implies that $A(\delta)$ holds. □

One additional simplification consists of checking $B(\delta)$ only for points $a, a' \in \partial F_{2k+1}(0)$. Define the condition

$$B^*(\delta) : \quad d_1(0, t) \leq d_{2k+1}(q, T_t q') + \delta \quad \forall q, q' \in \partial F_{2k+1}(0), |t| \in [\delta, \pi] \quad (\star)$$

Proposition 5.3. $B(\delta) \iff B^*(\delta)$.

Proof. We only need to prove that $B^*(\delta) \implies B(\delta)$. Notice that $B(\delta)$ is equivalent to

$$B''(\delta) : \quad d_1(0, t) \leq \min\{d_{2k+1}(q, T_t q'); q, q' \in F_{2k+1}(0)\} + \delta \quad \forall |t| \in [\delta, \pi]$$

and that

$$\min\{d_{2k+1}(q, T_t q'); q, q' \in F_{2k+1}(0)\} = \min\{d_{2k+1}(q, q'); q \in F_{2k+1}(0) \text{ and } q' \in F_{2k+1}(t)\}.$$

These imply the claim since $F_{2k+1}(0)$ (and therefore each fiber) is geodesically convex³ so that the minimum on the RHS is attained at boundary points. \square

As a consequence of Propositions 4.1, 5.2 and 5.3, we see that, in order to establish Conjecture 1, it suffices to establish $B^*(\delta)$ for $\delta = \delta_k = \frac{2\pi k}{2k+1}$.

5.3 Other results

In this section we introduce a convenient parameterization of odd-dimensional spheres and also explore some preliminary results.

5.3.1 Hopf coordinates on \mathbb{S}^{2k+1}

Hopf coordinates provide a well known coordinatization of $\mathbb{S}^3 \subset \mathbb{R}^4$ so that a point on \mathbb{S}^3 can be (uniquely) written as

$$q(\theta_1, \theta_2, \zeta) := (\cos(\theta_1) \cos(\zeta), \sin(\theta_1) \cos(\zeta), \cos(\theta_2) \sin(\zeta), \sin(\theta_2) \sin(\zeta)),$$

for $\theta_1, \theta_2 \in [0, 2\pi)$ and $\zeta \in [0, \frac{\pi}{2}]$. These coordinates are closely linked to the (topological) fact that \mathbb{S}^3 is homeomorphic to the topological join $\mathbb{S}^1 * \mathbb{S}^1$ of two copies of the circle; see Figure 4.

In general, since \mathbb{S}^{2k+1} is homeomorphic to the $(k+1)$ -fold join $\mathbb{S}^1 * \dots * \mathbb{S}^1$ ($k+1$ times), one would suspect that it is possible to generalize these coordinates to higher dimensional odd dimensional spheres. This is indeed the case; one can induce such coordinates as follows.

Firstly, consider k copies \mathbb{S}^1 labeled as $\mathbb{S}_{1,2}^1, \mathbb{S}_{3,4}^1, \dots, \mathbb{S}_{2i+1,2i+2}^1, \dots, \mathbb{S}_{2k+1,2k}^1$ such that the copy $\mathbb{S}_{2i+1,2i+2}^1$ lies in $\text{span}(e_{2i+1}, e_{2i+2})$ where $\{e_1, e_2, \dots, e_{2k+2}\}$ is canonical basis of \mathbb{R}^{2k+2} . Then, introduce $(\theta_1, \dots, \theta_{k+1}) \in [0, 2\pi)^{k+1}$ such that:

³For $t \neq 0$, the fiber $F_{2k+1}(t)$ can intersect $F_{2k+1}(0)$ only at boundary points.

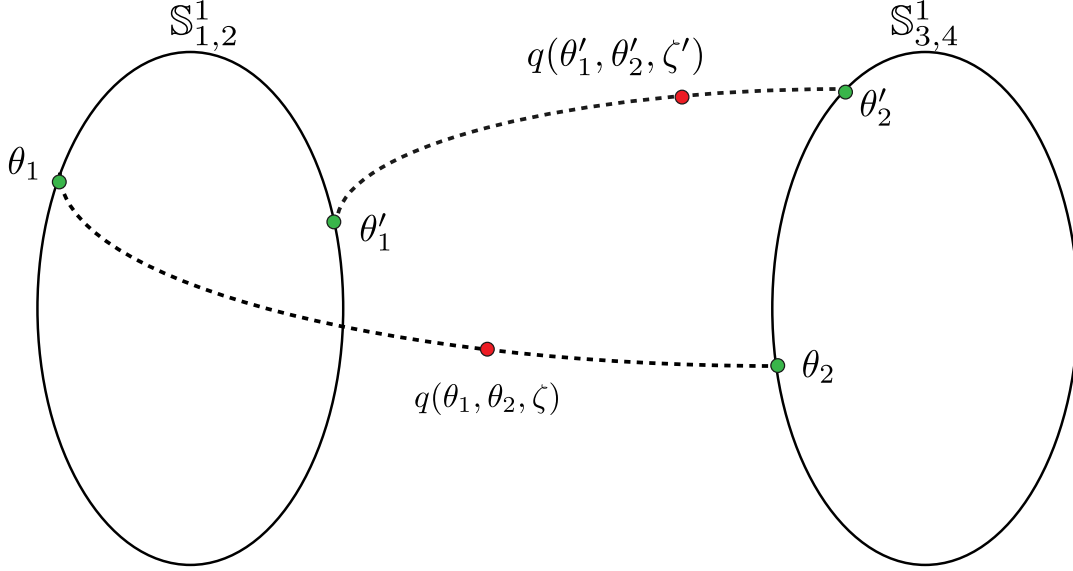


Figure 4: Hopf coordinates on \mathbb{S}^3 . See Section 5.3.1.

- $p_1 \in \mathbb{S}^1_{1,2}$ has coordinates $(\cos(\theta_1), \sin(\theta_1), 0, 0, \dots, 0)$ for $\theta_1 \in [0, 2\pi)$,
- $p_2 \in \mathbb{S}^1_{3,4}$ has coordinates $(0, 0, \cos(\theta_2), \sin(\theta_2), 0, 0, \dots, 0)$ for $\theta_2 \in [0, 2\pi)$,
- $p_i \in \mathbb{S}^1_{2i-1, 2i}$ has coordinates $(0, 0, 0, 0, \dots, 0, 0, \cos(\theta_i), \sin(\theta_i), 0, 0, \dots, 0)$ for $\theta_i \in [0, 2\pi)$,
- $p_{k+1} \in \mathbb{S}^1_{2k+1, 2k+2}$ has coordinates $(0, 0, \dots, 0, 0, \cos(\theta_k), \sin(\theta_k))$ for $\theta_{k+1} \in [0, 2\pi)$.

Secondly, consider $(a_1, a_2, \dots, a_i, \dots, a_{k+1}) \in [0, 1]^{k+1}$ such that $\sum_i a_i^2 = 1$.

Then, the Hopf coordinates of a point in \mathbb{S}^{2k+1} will be denoted by

$$q(p_1, \dots, p_{k+1}; a_1, \dots, a_{k+1})$$

or alternatively as

$$q(\theta_1, \dots, \theta_{k+1}; a_1, \dots, a_{k+1}).$$

Remark 5.4. The subsets $C(a_1, \dots, a_{k+1})$ of \mathbb{S}^{2k+1} obtained via the above parametrization for fixed a_1, \dots, a_{k+1} are analogues of the Clifford tori in \mathbb{S}^3 .

Directly from the definition of the rotation T_t in Section 5.1 and by the description of Hopf coordinates we obtain the following (using the notation established above).

Corollary 5.2. For all $t \in \mathbb{S}^1$,

$$T_t(q(\theta_1, \dots, \theta_i, \dots, \theta_{k+1}; a_1, \dots, a_i, \dots, a_{k+1})) = q(\theta_1 + t, \dots, \theta_i + (2i - 1)t, \dots, \theta_k + (2k + 1)t; a_1, \dots, a_i, \dots, a_k).$$

In particular, T_t does not affect the values of the coordinates a_1, \dots, a_{k+1} .

Using Hopf coordinates, for a given point $q = q(\theta_1, \dots, \theta_{k+1}; a_1, \dots, a_{k+1}) \in \mathbb{S}^{2k+1}$, we then define the following function $P_{2k+1}(\cdot; q) : (-\pi, \pi] \rightarrow \mathbb{R}$ given by

$$P_{2k+1}(t; q) := q \cdot \gamma_{2k+1}(t) = \frac{1}{\sqrt{k+1}} \sum_{\ell=0}^k a_\ell \cos((2\ell+1)t - \theta_{\ell+1}), \quad (2)$$

so that $d_{2k+1}(q, \gamma_{2k+1}(t)) = \arccos(P_{2k+1}(t; q))$.

5.3.2 Some properties of γ_{2k+1} and the TMC-EPC

The following conjecture is suggested by the overall goal of proving that the distortion of the TMC-EPC is minimal (see Conjecture 1). Recall the discussion in Section 3.1 which yields a lower bound for an EPC via the distortion of the embedding map and the covering radius of the projection $\Pi_{2k+1} : \mathbb{S}^{2k+1} \rightarrow \gamma_{2k+1}(\mathbb{S}^1)$:

$$\text{dis}(\psi_{2k+1}) \geq \max(\text{dis}(\gamma_{2k+1}), \rho(\Pi_{2k+1})). \quad (3)$$

Conjecture 5 (covering radius).

$$\rho(\Pi_{2k+1}) = \max_{q \in \mathbb{S}^{2k+1}} \min_{t \in \mathbb{S}^1} d_{2k+1}(q, \gamma_{2k+1}(t)) \leq \frac{\delta_k}{2} = \frac{\pi k}{2k+1}.$$

Remark 5.5. Note that the LHS $\rho(\Pi_{2k+1})$ is always bounded above by $\frac{\pi}{2}$. Indeed, if q is any point on \mathbb{S}^{2k+1} , then

$$d_{2k+1}(q, \gamma_{2k+1}(t)) + d_{2k+1}(q, -\gamma_{2k+1}(t)) = \pi$$

for every $t \in \mathbb{S}^1$. But, since $-\gamma_{2k+1}(t) = \gamma_{2k+1}(-t)$, the point q is at distance at most $\frac{\pi}{2}$ from the set $\{\gamma_{2k+1}(t), \gamma_{2k+1}(-t)\}$.

Remark 5.6. Experimentally, we've obtained the estimate $\rho(\Pi_3) \approx 0.9229$. Also, we've obtained the estimate $\text{dis}(\gamma_3) \simeq 0.8128$ (see Table 1). Using these, one obtains

$$d_{\text{GH}}(\mathbb{S}^1, \mathbb{S}^3) \leq \frac{1}{2} \text{dis}(\gamma_3) + d_{\text{H}}(\mathbb{S}^3, \gamma_3) \approx 1.3293$$

which is larger than the desired upper bound $\frac{\pi}{3} \approx 1.0472$.

In Section 7.2 we will suggest a strategy for approaching Conjecture 5 via the combinatorial structure of the so called Barvinok-Novik polytope (see Proposition 7.1).

Also motivated by Equation (3), the following proposition establishes that, when restricted to the image of $\gamma_{2k+1} \subset \mathbb{S}^{2k+1}$, the distortion of ψ_{2k+1} , does not exceed δ_k . This can be interpreted as a partial result towards Conjecture 1.

Note that, by definition of ψ_{2k+1} one has $F_{2k+1}(t) \cap \text{Im}(\gamma_{2k+1}) = \{\gamma_{2k+1}(t)\}$ for each $t \in \mathbb{S}^1$.

Proposition 5.4 (distortion of R_{2k+1} restricted to TMC). For all $s, t \in \mathbb{S}^1$ one has

$$|d_{2k+1}(\gamma_{2k+1}(s), \gamma_{2k+1}(t)) - d_1(s, t)| \leq \delta_k.$$

In other words,

$$\text{dis}(\gamma_{2k+1}) \leq \delta_k.$$

k	$\text{dis}(\gamma_{2k+1})$	$\frac{\delta_k}{2}$	δ_k
1	0.8128	1.0472	2.0944
2	1.1114	1.2566	2.5133
3	1.2694	1.3464	2.6928
4	1.3676	1.3963	2.7925
5	1.4345	1.4280	2.8560
6	1.4831	1.4500	2.8999

Table 1: Experimentally obtained values of $\text{dis}(\gamma_{2k+1})$ for several values of k . See Remark 5.7.

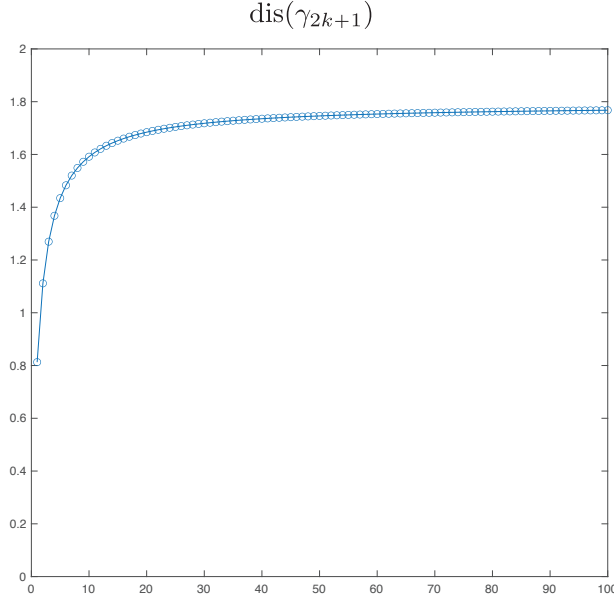


Figure 5: $\text{dis}(\gamma_{2k+1})$ as a function of k . See Remark 5.7

Remark 5.7. *The upper bound δ_k given above for $\text{dis}(\gamma_{2k+1})$ is not tight. For example, we can prove $\text{dis}(\gamma_3) \leq \frac{\pi}{3} = \frac{\delta_1}{2}$ \bullet . However, experimentally, we have verified that it is not true that $\text{dis}(\gamma_{2k+1}) \leq \frac{\delta_k}{2}$ for all k ; see Table 1 below, where this is violated for $k = 5, 6$. Our experiments (see Figure 5) also strongly suggest the following.*

Conjecture 6. $k \mapsto \text{dis}(\gamma_{2k+1})$ is monotonically increasing with k .⁴

The following function appears often in our considerations. For $t \in \mathbb{S}^{2k+1}$ let

$$h_k(t) := \gamma_{2k+1}(0) \cdot \gamma_{2k+1}(t) = \frac{1}{k+1} \sum_{\ell=0}^k \cos((2\ell+1)t). \quad (4)$$

Note that for $s, t \in \mathbb{S}^{2k+1}$,

$$d_{2k+1}(\gamma_{2k+1}(s), \gamma_{2k+1}(t)) = \arccos(h_k(s-t)).$$

Here we collect a number of useful properties of this function

⁴Our experiments indicate that $\text{dis}(\gamma_{2k+1})$ never exceeds ≈ 1.77 .

Proposition 5.5. 1. $h_k(t) = h_k(-t)$ for all $t \in \mathbb{S}^1$.

2. For $t \in [0, \pi]$ we have

$$h_k(t) = \begin{cases} \frac{1}{2^{(k+1)}} \frac{\sin(2^{(k+1)}t)}{\sin(t)} & \text{for } t \neq 0, \pi \\ 1 & \text{for } t = 0 \\ -1 & \text{for } t = \pi. \end{cases}$$

3. For all $t \in \mathbb{S}^1$,

$$\min_{\ell=0, \dots, k} \cos((2\ell + 1)t) \leq h_k(t) \leq \max_{\ell=0, \dots, k} \cos((2\ell + 1)t).$$

4. For $t \in [0, \delta_k]$,

$$h_k(t) \geq \cos(\delta_k).$$

The following lemma is elementary but useful.

Lemma 5.2. Let k be a non-negative integer. Then, for all $t, s \in \mathbb{S}^1$, we have

$$|d_1(s, t) - d_1((2k + 1)s, (2k + 1)t)| \leq \delta_k.$$

Proof of Proposition 5.4. The statement is equivalent to the condition

$$|d_{2k+1}(\gamma_{2k+1}(0), \gamma_{2k+1}(t)) - d_1(0, t)| \leq \delta_k$$

for all $t \in \mathbb{S}^1$. Note that

$$\cos(d_{2k+1}(\gamma_{2k+1}(0), \gamma_{2k+1}(t))) = h_k(t).$$

Therefore, by item 3 of Proposition 5.5,

$$\max_{\ell=0, \dots, k} \arccos(\cos((2\ell + 1)t)) \geq \arccos(h_k(t)) \geq \max_{\ell=0, \dots, k} \arccos(\cos((2\ell + 1)t)),$$

which is equivalent to

$$\max_{\ell=0, \dots, k} d_1(0, (2\ell + 1)t) \geq d_{2k+1}(\gamma_{2k+1}(0), \gamma_{2k+1}(t)) \geq \min_{\ell=0, \dots, k} d_1(0, (2\ell + 1)t).$$

The conclusion now follows from Lemma 5.2 and the fact that $\delta_\ell \leq \delta_k$ whenever $\ell \leq k$. For example, have have that the RHS above can be bounded as follows

$$\begin{aligned} \min_{\ell=0, \dots, k} d_1(0, (2\ell + 1)t) &\geq \min_{\ell=0, \dots, k} (d_1(0, t) - \delta_\ell) \\ &= d_1(0, t) - \max_{\ell=0, \dots, k} \delta_\ell \\ &= d_1(0, t) - \delta_k. \end{aligned}$$

□

Remark 5.8. Via Proposition 5.5, we have the following more or less explicit expression

$$\text{dis}(\gamma_{2k+1}) = \sup_{t \in (0, \pi)} |\arccos(h_k(t)) - t| = \sup_{t \in (0, \pi)} \left| \arccos \left(\frac{\sin(2(k+1)t)}{2(k+1)\sin(t)} \right) - t \right|.$$

Note that for $t = t_k := \frac{\pi}{2(k+1)}$ one has $h_k(t_k) = 0$, which implies that

$$\text{dis}(\gamma_{2k+1}) \geq \frac{\pi}{2} \frac{k}{k+1}.$$

It would be interesting to compute a more precise estimate of $\text{dis}(\gamma_{2k+1})$ \blacksquare .

Proof of Proposition 5.5. Item 1 is obvious. Item 2 follows via standard trigonometric manipulations (more precisely, through one of the so called Lagrange trigonometric identities). Item 3 is also obvious. \square

Proof of Lemma 5.2. It suffices to to prove the following two inequalities:

$$d_1((2k+1)t, 0) \leq d_1(t, 0) + \delta_k \text{ for } t \in [0, \pi - \delta_k] \quad (5)$$

and

$$d_1(t, 0) \leq d_1((2k+1)t, 0) + \delta_k \text{ for } t \in [\delta_k, \pi]. \quad (6)$$

Let's verify Equation (5) first. Note that, since $\pi - \delta_k = \frac{\pi}{2k+1}$, for $t \in [0, \pi - \delta_k]$ one has $(2k+1)t \in [0, \pi]$ and that $(2k+1)t \geq t$. Therefore (see Figure 6),

$$d_1((2k+1)t, 0) = d_1((2k+1)t, t) + d_1(t, 0) = 2kt + d_1(t, 0) \leq \frac{2k\pi}{2k+1} + d_1(t, 0) = \delta_k + d_1(t, 0).$$

Now we tackle Equation (6). In that case, write $t = \delta_k + \nu$ for $\nu \in [0, \pi - \delta_k]$. Then, $(2k+1)t = 2k\pi + (2k+1)\nu$ equals $(2k+1)\nu$ modulo 2π . Furthermore, given that $\nu \in [0, \pi - \delta_k]$, we have $(2k+1)\nu \in [0, \pi]$ and $(2k+1)\nu \geq \nu$. Hence, $d_1(t, 0) = \delta_k + \nu$ and $d_1((2k+1)t, 0) = (2k+1)\nu$ so that

$$d_1(t, 0) = \nu + \delta_k \leq (2k+1)\nu + \delta_k = d_1((2k+1)t, 0) + \delta_k.$$

\square

6 The case of \mathbb{S}^1 versus \mathbb{S}^3

We will use Hopf coordinates $(\theta_1, \theta_2, \zeta)$ on \mathbb{S}^3 so that a generic point on $\mathbb{S}^3 \subset \mathbb{R}^4$ can be written as

$$q(\theta_1, \theta_2, \zeta) := (\cos(\theta_1) \cos(\zeta), \sin(\theta_1) \cos(\zeta), \cos(\theta_2) \sin(\zeta), \sin(\theta_2) \sin(\zeta)),$$

for $\theta_1, \theta_2 \in [-\pi, \pi]$ and $\zeta \in [0, \frac{\pi}{2}]$. See Figure 4 for an illustration.

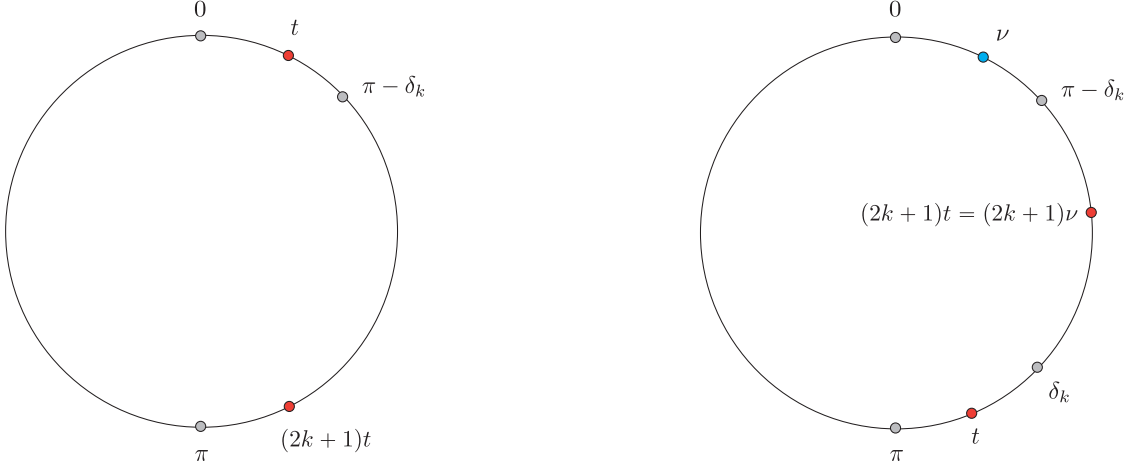


Figure 6: An illustration for the proof of Lemma 5.2. Left: the configuration corresponding to Equation (5). Right: the configuration corresponding to Equation (6).

6.1 Characterization of the fiber $F_3(0)$

We have a complete characterization of the fibers of R_3 .

Theorem 3. *We have*

$$\partial F_3(0) = \{q(\theta, 3\theta + \pi, \zeta(\theta)) \mid \theta \in [-\frac{\pi}{3}, \frac{\pi}{3}]\}$$

where

$$\zeta(\theta) := \operatorname{arccot}(3(3 - 4\sin^2(\theta))). \quad (7)$$

Furthermore, $F_3(0) = \operatorname{ConvSph}(\partial F_3(0))$, the geodesic convex hull of $\partial F_3(0)$.

See Figure 7 for a visualization of $F_3(0)$.

Remark 6.1. *As a consequence of Theorem 3, a generic point on $\partial F_3(0)$ has the following Hopf coordinates:*

$$\begin{aligned} \bar{q}(\theta) &:= q(\theta, 3\theta + \pi, \zeta(\theta)) \\ &= (\cos(\theta) \cos(\zeta(\theta)), \sin(\theta) \cos(\zeta(\theta)), \cos(3\theta + \pi) \sin(\zeta(\theta)), \sin(3\theta + \pi) \sin(\zeta(\theta))) \\ &= (\cos(\theta) \cos(\zeta(\theta)), \sin(\theta) \cos(\zeta(\theta)), -\cos(3\theta) \sin(\zeta(\theta)), -\sin(3\theta) \sin(\zeta(\theta))) \end{aligned}$$

for $\theta \in [-\frac{\pi}{3}, \frac{\pi}{3}]$.

Remark 6.2. *Using the parametrization of $\partial F_3(0)$ given by Theorem 3 we can consider the function*

$$[-\frac{\pi}{3}, \frac{\pi}{3}] \ni \theta \mapsto \rho_3(\theta) := d_3(\bar{q}(\theta), \gamma_3(0)) = \arccos(\bar{q}(\theta) \cdot \gamma_3(0))$$

and find its maximum value. A plot of $\rho_3(\theta)$ for $\theta \in [-\frac{\pi}{3}, \frac{\pi}{3}]$ is shown in Figure 8. Numerically, we determined that the maximum value of ρ_3 is ≈ 0.9232 , which is strictly smaller than the upper bound $\frac{\pi}{3}$ implied by Proposition 7.1. The minimum value is ≈ 0.6476 .

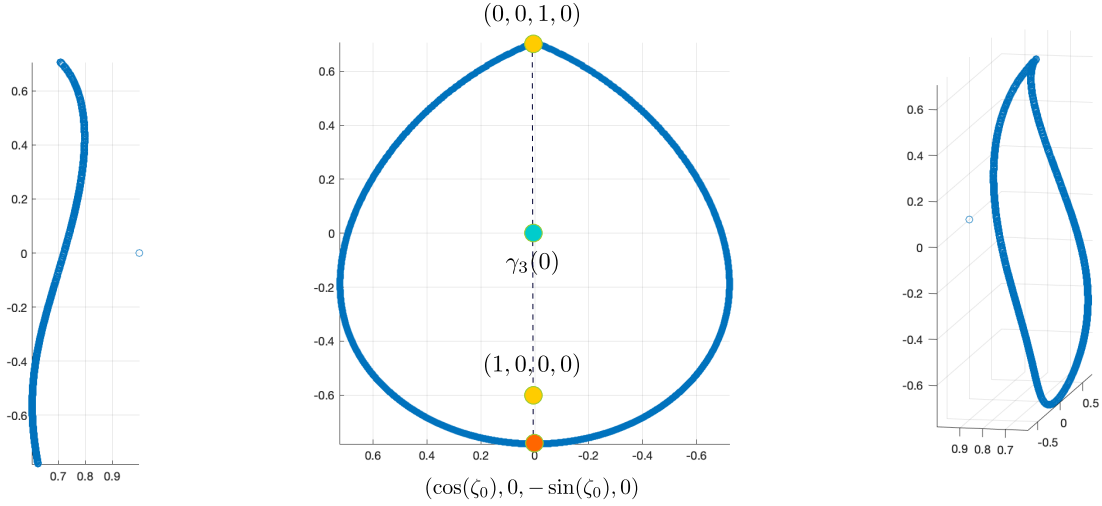


Figure 7: Three views of the boundary of the fiber $F_3(0)$; see Theorem 3. The center figure shows the the points $\mathbb{S}_{3,4}^1 \ni (0, 0, 1, 0) = \bar{q}(\pm\frac{\pi}{3})$, $(\cos(\zeta_0), 0, -\sin(\zeta_0), 0) = \bar{q}(0)$ (where $\zeta_0 := \operatorname{arccot}(9)$) both lying on $\partial F_3(0)$ together with the points $\gamma_3(0) = \frac{1}{\sqrt{2}}(1, 0, 1, 0)$ and $\mathbb{S}_{1,2}^1 \ni (1, 0, 0, 0)$ both lying in the interior of $F_3(0)$; see Figure 4.

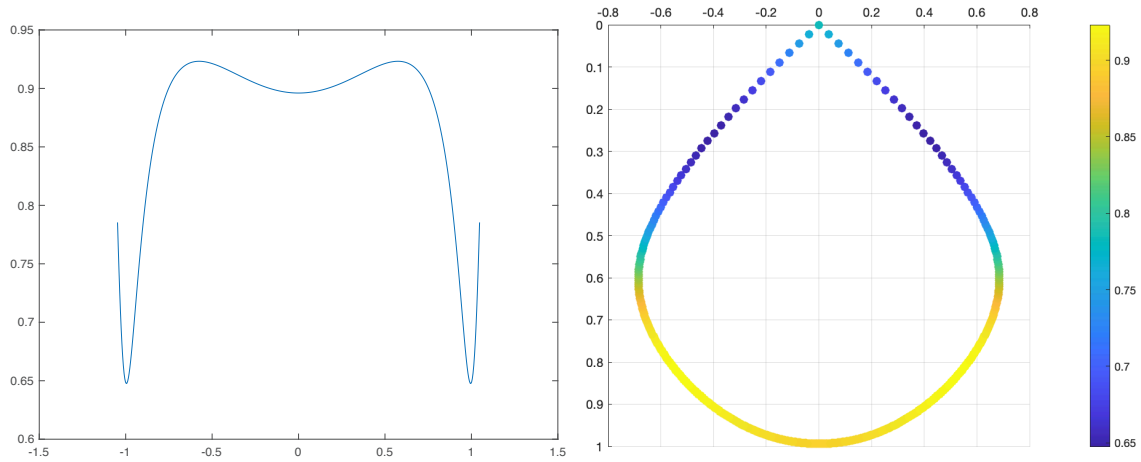


Figure 8: **Left:** Plot of $\rho_3(\theta) := d_3(\bar{q}(\theta), \gamma_3(0))$ for $\theta \in [-\frac{\pi}{3}, \frac{\pi}{3}]$; see Remark 6.2. The maximum value of ρ_3 is approximately 0.9232 whereas the minimum value is ≈ 0.6476 . **Right:** Plot of $\partial F_3(0)$ colored by values of ρ_3 .

Lemma 6.1. Let $\zeta \in [0, \frac{\pi}{2}]$ and $\theta \in [-\pi, \pi)$. Consider the trigonometric function

$$P_{\zeta, \theta} : [-\pi, \pi) \rightarrow \mathbb{R}$$

defined by

$$P_{\zeta, \theta}(t) := \cos(\zeta) \cos(t) + \sin(\zeta) \cos(3t - \theta)$$

and let $M(P_{\zeta, \theta})$ denote the set of all global maxima points of $P_{\zeta, \theta}$. Then,

- $M(P_{\zeta, \theta}) \subset [-\frac{\pi}{3}, \frac{\pi}{3}]$ whenever $\zeta \in [0, \frac{\pi}{2})$.
- $|M(P_{\zeta, \theta})| = 2$ precisely when $\theta = \pm\pi$ and $\zeta \in (\zeta_0, \frac{\pi}{2})$, where $\zeta_0 := \operatorname{arccot}(9)$.
- $|M(P_{\zeta, \theta})| = 3$ precisely when $\zeta = \frac{\pi}{2}$.
- $|M(P_{\zeta, \theta})| = 1$ in all other cases.

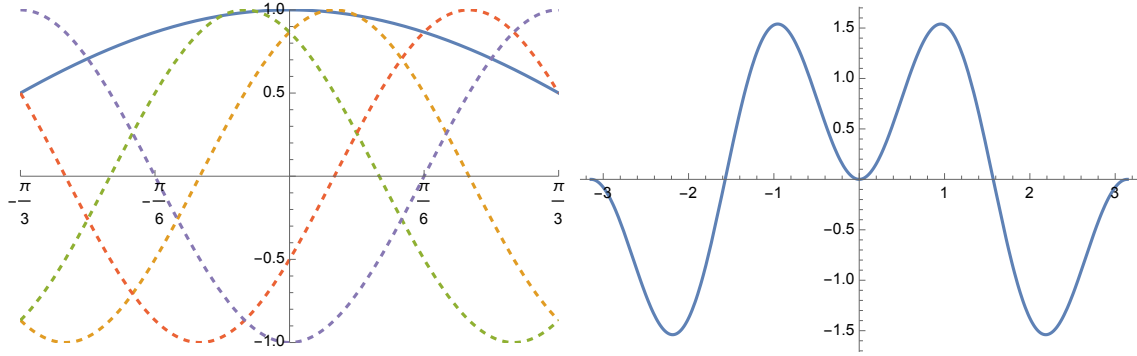


Figure 9: See the proof of Lemma 6.1. **Left:** The solid line is the plot of $\cos(t)$ for $t \in [-\frac{\pi}{3}, \frac{\pi}{3}]$. Dashed lines correspond to plots of $\cos(3t - \theta)$ for different choices of θ . **Right:** Plot of $\sqrt{2} P_{\zeta, \pm\pi}(t) = \cos(t) - \cos(3t)$, $t \in [-\pi, \pi]$, for $\zeta = \frac{\pi}{4}$.

Proof. We first establish the following.

Claim 6.1. When $\zeta \in [0, \frac{\pi}{2})$, all global maxima points of $P_{\zeta, \theta}$ are attained inside of the interval $I_0 := [-\frac{\pi}{3}, \frac{\pi}{3}]$.

To prove this claim, note that $[-\pi, \pi) = I_- \cup I_0 \cup I_+$ where $I_+ = (\frac{\pi}{3}, \pi)$ and $I_- = [-\pi, -\frac{\pi}{3})$. Let $g(t) := \cos(\zeta) \cos(t)$ and $h(t) := \sin(\zeta) \cos(3t - \theta)$. Note that:

$$g(s) > g(s - \frac{2\pi}{3}) \quad \text{for all } s \in [-\frac{\pi}{3}, \frac{\pi}{3}) \quad (8)$$

$$g(s) > g(s + \frac{2\pi}{3}) \quad \text{for all } s \in (-\frac{\pi}{3}, \frac{\pi}{3}]. \quad (9)$$

See Figure 9. The claim follows from the following two items:

- If $t \in I_+$, then $s := t - \frac{2\pi}{3} \in (-\frac{\pi}{3}, \frac{\pi}{3}) \subset I_0$. Thus

$$P_{\zeta, \theta}(t) = g(t) + h(t) = g(t) + h(t - \frac{2\pi}{3}) = g(s + \frac{2\pi}{3}) + h(s) < P_{\zeta, \theta}(s) = P_{\zeta, \theta}(t - \frac{2\pi}{3}),$$

where the last inequality is due to Equation (9).

- If $t \in I_-$, then $s := t + \frac{2\pi}{3} \in [-\frac{\pi}{3}, \frac{\pi}{3}) \subset I_0$. Thus

$$P_{\zeta,\theta}(t) = g(t) + h(t) = g(t) + h(t + \frac{2\pi}{3}) = g(s - \frac{2\pi}{3}) + h(s) < P_{\zeta,\theta}(s) = P_{\zeta,\theta}(t + \frac{2\pi}{3}),$$

where the last inequality is due to Equation (8).

Assuming $\zeta \in [0, \frac{\pi}{2})$, given Claim 6.1 above, in order for $P_{\zeta,\theta}$ to have more than one global maximum inside of I_0 , the function h must have at least two local maxima or two local minima in I_0 . But this requires $\theta = \pm\pi$. Under this assumption, $P_{\zeta,\pm\pi}(t) = \cos(\zeta)\cos(t) - \sin(\zeta)\cos(3t)$ so that $P'_{\zeta,\pm\pi}(t) = -\cos(\zeta)\sin(t) + 3\cos(\zeta)\sin(3t)$. See Figure 9. Since $\sin(3t) = \sin(t)(3 - 4\sin^2(t))$, the critical points inside I_0 are therefore $t = 0$ together with $t_{\pm}(\zeta)$, the solutions of the equation

$$4\sin^2(t) = 3 - \frac{\cot(\zeta)}{3}. \quad (10)$$

Since $P''_{\zeta,\pi}(0) = -\cos(\zeta) + 9\sin(\zeta)$, $t = 0$ will correspond to a local minimum whenever $\cot(\zeta) < 9$ and it will correspond to a global maximum when $\cot(\zeta) \geq 9$. For Equation (10) to have two different solutions $t_{\pm}(\zeta)$ inside the interval I_0 it is necessary and sufficient that $\cot(\zeta) < 9$. Whenever this condition holds, $t_{\pm}(\zeta)$ will be two (different) global maxima points. Finally, when $\zeta = \zeta_0 = \operatorname{arccot}(9)$, $t = 0$ will be the sole global maximum in I_0 and $P'_{\zeta_0,\pm\pi}$ will have a triple root at $t = 0$.

It remains to analyze the case $\zeta = \frac{\pi}{2}$. In this case, $P_{\frac{\pi}{2},\theta}(t) = \cos(3t - \theta)$, which certainly has exactly three different global maxima points. \square

Proof of Theorem 3. Any point $q(\theta_1, \theta_2, \zeta)$ lying on the boundary of $F_3(0)$ will have more than one closest point in γ_3 .⁵ This means that the function $P_3 : [-\pi, \pi) \rightarrow \mathbb{R}$ defined as

$$P_3(t) := q(\theta_1, \theta_2, \zeta) \cdot \gamma_3(t) = \cos(t - \theta_1) \frac{\cos(\zeta)}{\sqrt{2}} + \cos(3t - \theta_2) \frac{\sin(\zeta)}{\sqrt{2}}$$

will have at least one global maximum, in addition to $t = 0$.

With the notation of Lemma 6.1,

$$P_3(t) = \frac{1}{\sqrt{2}} P_{\zeta,\theta}(t - \theta_1) \text{ for } \theta := \theta_2 - 3\theta_1.$$

Taking into account the considerations above, by Lemma 6.1, we must have that $\zeta > \zeta_0$, $\theta_2 = 3\theta_1 \pm \pi$ and that, for any such global maximum, $t - \theta_1 \in [-\frac{\pi}{3}, \frac{\pi}{3}]$. This has to be the case for $t = 0$ which gives the following relationship between θ_1 and θ_2 :

$$\theta_2 = 3\theta_1 \pm \pi \text{ for } \theta_1 \in [-\frac{\pi}{3}, \frac{\pi}{3}]. \quad (11)$$

On the other hand, note that by Proposition 5.1 we must have

$$F_3(0) \subset \{v \in \mathbb{R}^4 \mid v \cdot \dot{\gamma}_3(0) = 0\} = \Sigma_0.$$

⁵That, is there will be at least one point γ_3 different from γ_0 that is closest to $q(\theta_1, \theta_2, \zeta)$.

Since $\dot{\gamma}_3(0) = \frac{1}{\sqrt{2}}(0, 1, 0, 3)$, every point (x, y, z, w) in the hyperplane Σ_0 satisfies $y + 3w = 0$. For a point $q(\theta_1, \theta_2, \zeta)$ in $\mathbb{S}^3 \cap \Sigma_0$, expressed in Hopf coordinates, this gives the condition

$$\sin(\theta_1) \cos(\zeta) + 3 \sin(\theta_2) \sin(\zeta) = 0. \quad (12)$$

By Equation (11), if $q(\theta_1, \theta_2, \zeta)$ is in $\partial F_3(0)$, we have that $\theta_2 = 3\theta_1 \pm \pi$ so that Equation (12) becomes

$$\sin(\theta_1) \cos(\zeta) = 3 \sin(3\theta_1) \sin(\zeta).$$

Via the formula $\sin(3\alpha) = \sin(\alpha)(3 - 4\sin^2(\alpha))$ we obtain from the above condition that

$$\cos(\zeta) = 3(3 - 4\sin^2(\theta_1)) \sin(\zeta)$$

from which the first claim follows. The second claim follows from Proposition 5.1. \square

6.2 The modulus of discontinuity of ψ_3 is minimal

By combining Corollary 5.1 with Theorem 3 and Theorem 2 we have that the modulus of discontinuity of ψ_3 is minimal.

Theorem 4. $\text{disc}(\psi_3) = \frac{2\pi}{3}$.

Indeed, this theorem is proved by directly exploiting the precise description of $\partial F_3(0)$ given by Theorem 3. Since, by Proposition 2.1, distortion is always lower bounded by modulus of discontinuity, Theorem 4 can be seen as a preamble to and a consequence of Theorem 5 below. We however include a standalone proof here because this proof contains interesting ideas related to the effect of the rotation T_t on $\partial F_3(0)$. This theorem will be generalized, via completely different arguments, in Theorem 9. The arguments therein exploit a connection between the Voronoi cells induced by γ_{2k+1} and known results about the facial structure of the Barvinok-Novik polytope.

Proof of Theorem 4. By Theorem 2, it suffices to prove that $\text{disc}(\psi_3) \leq \frac{2\pi}{3}$.

Assume that $q_0 \in \partial F(0) \cap \partial F(t)$ for some $t \in [0, \pi]$. Then, we have:

- Since, by Remark 5.1, $\partial F(t) = T_t(\partial F(0))$, there exists $q'_0 \in \partial F(0)$ such that $q_0 = T_t(q'_0)$.
- By Remark 6.1, there exist $\theta_0, \theta'_0 \in [-\frac{\pi}{3}, \frac{\pi}{3})$ such that

$$q_0 = q(\theta_0, 3\theta_0 + \pi, \zeta(\theta_0)) \text{ and } q'_0 = q(\theta'_0, 3\theta'_0 + \pi, \zeta(\theta'_0)).$$

- By Corollary 5.2 we have

$$q_0 = T_t(q'_0) = T_t(q(\theta'_0, 3\theta'_0 + \pi, \zeta(\theta'_0))) = q(\theta'_0 + t, 3\theta'_0 + \pi + 3t, \zeta(\theta'_0)).$$

Hence, through the equality

$$q(\theta_0, 3\theta_0 + \pi, \zeta(\theta_0)) = q_0 = q(\theta'_0 + t, 3\theta'_0 + \pi + 3t, \zeta(\theta'_0))$$

we see that the following two conditions must hold: $\theta_0 = \theta'_0 + t$ and $\zeta(\theta_0) = \zeta(\theta'_0)$. Via the explicit expression for $\zeta(\cdot)$ given in Equation (7), we see that the second condition implies that it must then hold that $\theta_0 = \pm\theta'_0$. The case $\theta_0 = \theta'_0$ leads to $t = 0$ via the first condition. The case $\theta_0 = -\theta'_0$ gives $\theta'_0 = -\frac{t}{2}$.

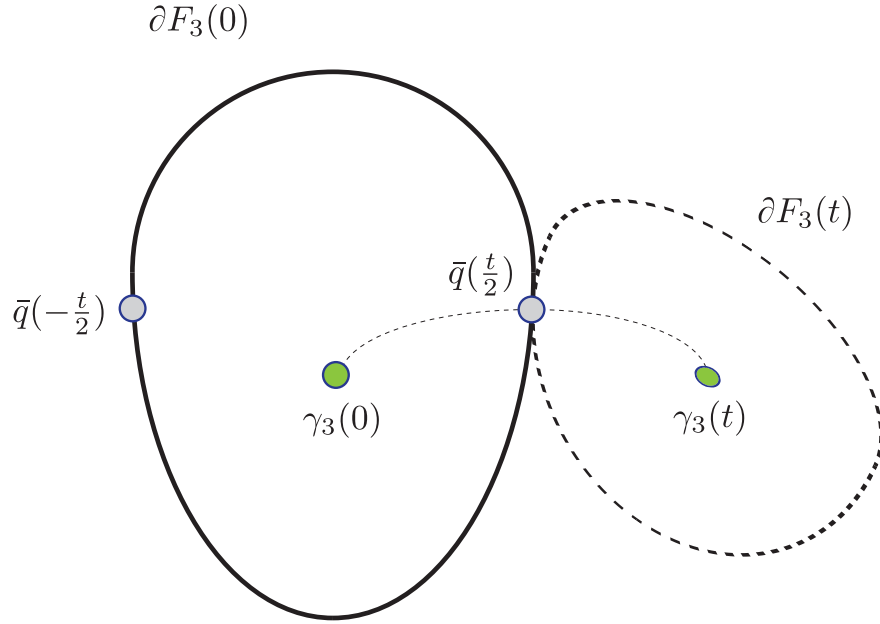


Figure 10: The point $\bar{q}(\frac{t}{2})$ is in the intersection $\partial F_3(0) \cap \partial F_3(t)$; see the proof of Theorem 4.

- Finally, the condition that $\theta'_0 \in [-\frac{\pi}{3}, \frac{\pi}{3})$ yields that it must be that $t \leq \frac{2\pi}{3}$. In other words, $q_0 = \bar{q}(\frac{t}{2})$ and $q'_0 = \bar{q}(-\frac{t}{2})$; see Figure 10.

□

6.3 The distortion of R_3 is minimal

Exploiting the characterization of $F_3(0)$ established in Theorem 3 we now have the following result.

Theorem 5. $\text{dis}(R_3) \leq \frac{2\pi}{3}$.

Via ideas described in Section 5.2 and Theorem 3, the proof is reduced to checking two inequalities involving elementary trigonometric functions which can we verify with the aid of a computer program.⁶

Computer assisted proof . Given the above, it is enough to verify condition $B^*(\frac{2\pi}{3})$ (from Equation (\star)), that is:

$$d_1(0, t) - \frac{2\pi}{3} \leq d_3(q, T_t q') \quad \forall q, q' \in \partial F_3(0), |t| \in [\frac{2\pi}{3}, \pi].$$

For $t \in [\frac{2\pi}{3}, \pi]$, this is equivalent to the condition

$$(*) \quad \cos(t - \frac{2\pi}{3}) \geq q \cdot T_t q' \quad \forall q, q' \in \partial F_3(0), |t| \in [\frac{2\pi}{3}, \pi].$$

⁶We use the term “computer assisted proof” for lack of a better one.

Since the RHS involves points on $q, q' \in \partial F_3(0)$, via Remark 6.1, writing $q = q(\theta)$ and $q' = q(\theta')$, we see that

$$q \cdot T_t q' = F_t(\theta, \theta') := \cos(\theta - \theta' + t) \cos(\zeta) \cos(\zeta') + \cos(3(\theta - \theta' + t)) \sin(\zeta) \sin(\zeta')$$

where we've written $\zeta := \zeta(\theta)$ and $\zeta' := \zeta(\theta')$ for conciseness. Condition (*) is therefore equivalent to the following condition involving elementary functions

$$(**) \quad \cos(t - \frac{2\pi}{3}) \geq F_t(\theta, \theta') \quad \forall \theta, \theta' \in [-\frac{\pi}{3}, \frac{\pi}{3}], t \in [\frac{2\pi}{3}, \pi].$$

Analogously, the case $t \in [-\pi, -\frac{2\pi}{3}]$ leads to the condition

$$(***) \quad \cos(t + \frac{2\pi}{3}) \geq F_t(\theta, \theta') \quad \forall \theta, \theta' \in [-\frac{\pi}{3}, \frac{\pi}{3}], t \in [-\pi, -\frac{2\pi}{3}].$$

These two conditions involving elementary functions were verified with the assistance of Matlab [MS23, Function TestIneqR3.m]. \square

7 The case \mathbb{S}^1 versus \mathbb{S}^{2k+1}

In this section we describe some results for the case of \mathbb{S}^1 versus \mathbb{S}^{2k+1} which are applicable to the case $k \geq 2$.

7.1 Connections to the Barvinok-Novik polytope

The convex hull of the image of the TMC is nowadays known as the *Barvinok-Novik polytope*. It is defined as

$$\mathcal{B}_{2k} := \text{Conv}(\gamma_{2k-1}(\mathbb{S}^1)).$$

In Section 7.2 below we will use results about the facial structure of this polytope to establish some results pertaining to the TMC-EPCs.

Smilansky [Smi90] studied \mathcal{B}_4 and Barvinok and Novik [BN08], and then Vinzant [Vin11] and Barvinok-Lee-Novik [BLN13] studied the general case; see also [Bar17].

Smilansky obtained the following⁷ characterization of the facial structure of \mathcal{B}_4 .

Theorem 6 ([Smi90, Theorem 1] and [BN08, Theorem 4.1]). *The proper faces of \mathcal{B}_4 are*

- (0) the 0-dimensional faces (vertices) are $\gamma_3(t)$ for $t \in \mathbb{S}^3$.
- (1) the 1-dimensional faces (edges) are the segments

$$[\gamma_3(t_1), \gamma_3(t_2)]$$

where $t_1 \neq t_2$ and $d_1(t_1, t_2) \leq \frac{2\pi}{3}$; and

- (2) the 2-dimensional faces of \mathcal{B}_4 are all the equilateral triangles

$$\Delta_t := \text{Conv}(\gamma_3(t), \gamma_3(t - \frac{2\pi}{3}), \gamma_3(t + \frac{2\pi}{3})), t \in \mathbb{S}^1.$$

⁷Smilansky's results are more general than what we state here.

Whereas a complete characterization of the facial structure of \mathcal{B}_{2k} for general k does not seem to be yet available [Bar17, Section 2],⁸ the following result provides a complete description of its edges.

Theorem 7 ([BN08, Theorem 1.1] and [Vin11, Theorem 1]). *For $t_1 \neq t_2$ in \mathbb{S}^1 , the segment $[\gamma_{2k-1}(t_1), \gamma_{2k-1}(t_2)]$ is an exposed edge of \mathcal{B}_{2k} if and only if $d_1(t_1, t_2) \leq \delta_{k-1}$.*

The following result provides partial information on higher dimensional faces.

Theorem 8 ([BN08, Theorem 1.2] and [BLN13, Theorem 1.1]). *For every k there exists a number $\pi > \phi_k > \frac{\pi}{2}$ such that if $\ell \leq k$ and $A = \{t_1, \dots, t_\ell\} \subset \mathbb{S}^1$ are ℓ distinct points contained in an arc with length at most ϕ_k , then $\text{Conv}(\gamma_{2k-1}(A))$ is an $(\ell - 1)$ -dimensional exposed face of \mathcal{B}_{2k} .*

Remark 7.1. *Certainly, through Theorem 6, $\phi_2 = \frac{2\pi}{3}$. The authors of [BLN13] verified that:*

- $\lim_k \phi_k = \frac{\pi}{2}$,
- $\phi_3 = \pi - \arccos\left(\frac{3-\sqrt{5}}{2}\right)$,

and also determined the precise value of ϕ_4 .

Remark 7.2 (A family of simplicial faces). *In [BN08, page 86] Barvinok and Novik also describe the following 1-parameter family of $(2k - 1)$ -dimensional simplicial faces of \mathcal{B}_{2k} :*

$$\Delta_t := \text{Conv}\left(T_t(\gamma_{2k-1}(Q_{2k-1}))\right), \text{ where } Q_{2k-1} := \left\{0, \frac{2\pi}{2k-1}, \dots, \frac{2\pi(2k-2)}{2k-1}\right\}$$

are the vertices of a regular odd polygon inscribed in \mathbb{S}^1 . The authors observe that, due to properties of the TMC, Δ_t is a $(2k - 2)$ -dimensional regular simplex.

In [Sin13, Proposition 5.2] the author establishes that, in fact, all faces of \mathcal{B}_{2k} are simplicial. Combining this with Theorem 7 we obtain the following.

Corollary 7.1. *Every face σ of \mathcal{B}_{2k} is a simplex of the form $\sigma = \text{Conv}(\gamma_{2k-1}(A))$ for some finite subset $A \subset \mathbb{S}^1$ such that $\text{diam}(A) \leq \delta_{k-1}$.*

7.2 An application to Conjecture 5

Note that the boundary $\partial\mathcal{B}_{2k+2}$ is homeomorphic to \mathbb{S}^{2k+1} and its projection onto \mathbb{S}^{2k+1} gives a simplicial decomposition \mathfrak{D}_{2k+1} of \mathbb{S}^{2k+1} ,

$$\mathbb{S}^{2k+1} = \bigcup_{\sigma \in \mathfrak{D}_{2k+1}} \sigma,$$

into geodesic (and therefore convex) simplices of different dimensions. This then suggests that, in order to tackle Conjecture 5, one could exploit the precise description of the cells given by Theorem 6, Theorem 7, Theorem 8 and Remark 7.2 in order to verify

$$\min_{t \in \mathbb{S}^1} d_{2k+1}(q, \gamma_{2k+1}(t)) \leq \frac{\delta_k}{2} \text{ for all } q \in \sigma \in \mathfrak{D}_{2k+1}.$$

⁸Barvinok notes “For larger $[k]$, we have only some fragmentary information regarding the facial structure of the convex hull of $\dots[\gamma_{2k+1}]$.”

Using this strategy we are able to establish Conjecture 5 for the case $k = 1$. We also provide partial information about other cases which could be useful as more information becomes available regarding the faces of the Barvikov-Novik polytope. Some of the arguments in the proof of Proposition 7.1 can be generalized beyond the case $k = 1$.

Proposition 7.1. *For all $q \in \mathbb{S}^3$ one has*

$$\min_{t \in \mathbb{S}^1} d_3(q, \gamma_3(t)) \leq \frac{\pi}{3}.$$

Lemma 7.1 (🔴). *For all $q \in \sigma \in \mathfrak{D}_{2k+1}$, where σ has dimension 1, one has*

$$\min_{t \in \mathbb{S}^1} d_{2k+1}(q, \gamma_{2k+1}(t)) \leq \frac{\delta_k}{2}.$$

Proof. According to Theorem 7, any such σ is a geodesic segment joining $\gamma_{2k+1}(t)$ and $\gamma_{2k+1}(s)$, where $d_1(t, s) \leq \frac{2\pi}{3}$. Any q on that segment will be at distance at most

$$\mu_k(t, s) := \frac{1}{2} d_{2k+1}(\gamma_{2k+1}(t), \gamma_{2k+1}(s))$$

from the set consisting of the two endpoints of the geodesic segment. Then, via item 4 of Proposition 5.5, we have

$$\min_{\tau \in I} h_k(\tau) \geq \cos(\delta_k)$$

which implies that, for $t, s \in \mathbb{S}^1$ such that $d_1(t, s) \leq \delta_k$,

$$\mu_k(t, s) \leq \frac{1}{2} \arccos \left(\min_{\tau \in I} h_k(\tau) \right) \leq \frac{1}{2} \delta_k.$$

□

Proof of Proposition 7.1. According to Corollary 7.1, \mathbb{S}^3 can be decomposed into simplicial cells $\sigma \in \mathfrak{D}_3$ of dimension at most 2 such that $\sigma = \text{Conv}(\gamma_3(A))$, where A is a subset of \mathbb{S}^1 with diameter at most $\delta_1 = \frac{2\pi}{3}$. Note that the cardinality of S can be at most 3. We now consider the following cases:

- dimension zero cells corresponding to points lying on γ_3 ;
- dimension one cells: geodesic segments joining points $\gamma_3(t)$ and $\gamma_3(s)$ s.t. $d_1(t, s) \leq \frac{2\pi}{3}$;
- dimension 2 cells: regular spherical simplices arising as the projection on \mathbb{S}^3 of the equilateral triangles determined by triples of points of the form $\gamma_3(t)$, $\gamma_3(t + \frac{2\pi}{3})$ and $\gamma_3(t - \frac{2\pi}{3})$.

The second case can be dealt via Lemma 7.1 (for $k = 1$). The third case leads to considering, for each $t \in \mathbb{S}^1$, the point inside the aforementioned spherical equilateral triangle that is as far as possible from its vertices. This point will be the center $(0, 0, \cos(3t), \sin(3t))$ of the triangle and this point is at distance $\arccos \left(\frac{1}{\sqrt{2}} \right) = \frac{\pi}{4} < \frac{\pi}{3}$ from the vertices. □

In Section 7 we provide a precise connection between the facial structure $\mathcal{B}_{2k+2}(\mathcal{D}_{2k+1})$ and the Voronoi tiling of \mathbb{S}^{2k+1} induced by the TMC.

7.3 Connecting structure of \mathcal{B}_{2k} to Voronoi tiling induced by γ_{2k+1}

The following proposition establishes a duality between the facial structure of $\mathcal{B}_{2(k+1)}$ and the Voronoi tiling of \mathbb{S}^{2k+1} induced by γ_{2k+1} .

Proposition 7.2. *Let $t_1, t_2, \dots, t_\ell \in \mathbb{S}^1$ be distinct points. Then,*

$$\bigcap_{i=1}^{\ell} \partial F_{2k+1}(t_i) \neq \emptyset \iff \text{Conv}(\{\gamma_{2k+1}(t_1), \dots, \gamma_{2k+1}(t_\ell)\}) \text{ is an exposed face of } \mathcal{B}_{2(k+1)}.$$

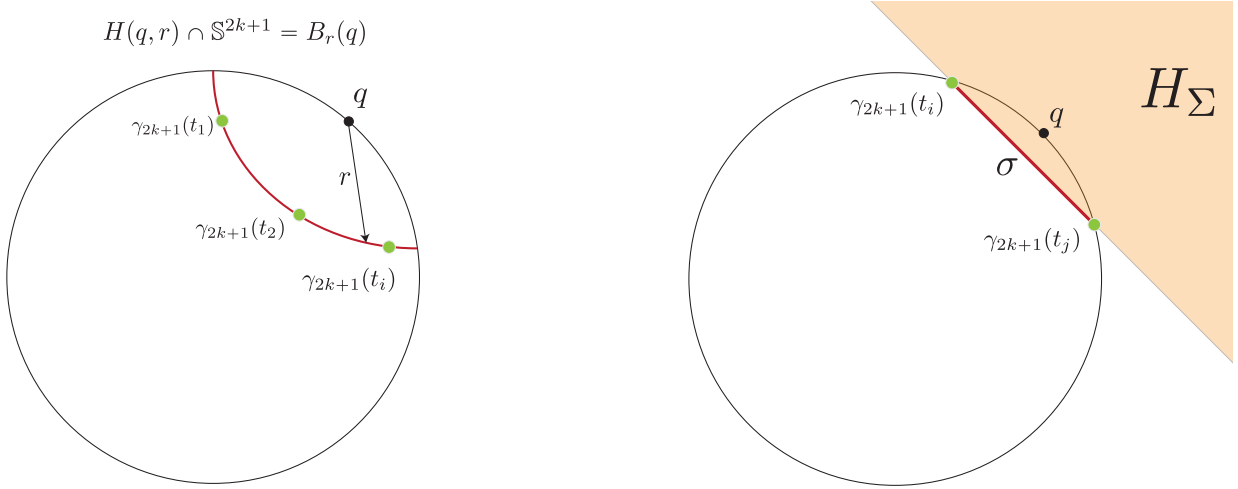


Figure 11: See the proof of Proposition 7.2. **Left:** the point $q \in \partial F_{2k+1}(t_i)$ is equidistant to all $\gamma_{2k+1}(t_i)$. The red line represents the boundary of the spherical cap (geodesic ball) $B_r(q) = H(q, r) \cap \mathbb{S}^{2k+1}$. **Right:** σ is an exposed face of $\mathcal{B}_{2(k+1)}$. The intersection $H_\Sigma \cap \mathbb{S}^{2k+1}$ is a spherical cap.

Remark 7.3 (🕒). *Note that Lemma 6.1 (or alternatively, Theorem 3) together with Proposition 7.2 permits recovering Theorem 6 which provides a complete characterization of \mathcal{B}_4 . The duality between the intersection pattern of Voronoi cells and the facial structure of the Barvinok-Novik polytope seems to be an interesting direction to further explore. In particular, the current partial knowledge about the facial structure of \mathcal{B}_{2k+2} can be utilized to shed light on the structure of $\partial F_{2k+1}(0)$. On the other hand, the fact that currently the full characterization of the facial structure of \mathcal{B}_6 is not known suggests that determining the precise shape of $\partial F_5(0)$ might pose some challenges. One expects these challenges to be present in terms of determining the shape of $\partial F_{2k+1}(0)$ for all $k \geq 2$.*

Remark 7.4. *The connection between the convex hull $\text{Conv}(A)$ of a finite subset A of \mathbb{S}^n and the Voronoi tiling of \mathbb{S}^n it induces already appears in the PhD thesis of Brown [Bro79a]; see also [Bro79b, For17]. We include a proof of Proposition 7.2 for completeness since this equivalence might not be well known.*

The following corollary to Theorem 7 and Proposition 7.2 will be immediately useful.

Corollary 7.2. For all $t, s \in \mathbb{S}^1$,

$$\partial F_{2k+1}(s) \cap F_{2k+1}(s) \neq \emptyset \iff d_1(s, t) \leq \delta_k.$$

Proof of Proposition 7.2. Suppose that $q \in \partial F_{2k+1}(t_i)$ for $i = 1, \dots, \ell$. This implies that q is equidistant to all $\gamma_{2k+1}(t_i)$. Let $r := d_{2k+1}(q, \gamma_{2k+1}(t_i))$ be the value of the common distance. Then, the open geodesic ball $B_r(q)$ does not contain any point $\gamma_{2k+1}(t)$, $t \in \mathbb{S}^1$, in its interior. Since $B_r(q)$ is the intersection of \mathbb{S}^{2k+1} with the following half-space (see the left panel of Figure 11)

$$H(q, r) := \{x \in \mathbb{R}^{2k+2} \mid (x - q \cos(r)) \cdot q \geq 0\},$$

we have that $\text{Conv}(\{\gamma_{2k+1}(t_1), \dots, \gamma_{2k+1}(t_\ell)\})$ is an exposed face of $\mathcal{B}_{2(k+1)}$.

For the converse, assume that $\sigma = \text{Conv}(\{\gamma_{2k+1}(t_1), \dots, \gamma_{2k+1}(t_\ell)\})$ is an exposed face of $\mathcal{B}_{2(k+1)}$. Let Σ be a supporting hyperplane for this face, let H_Σ be the associated half-space such that $\mathcal{B}_{2(k+1)} \cap H_\Sigma = \sigma$ and let q be the center of the spherical cap $\mathbb{S}^{2k+1} \cap H_\Sigma$; see the right panel of Figure 11. Let r be the (spherical) radius of this cap, i.e. such that $\mathbb{S}^{2k+1} \cap H_\Sigma = \overline{B_r(q)}$. Then, by construction, q is at distance r to $\gamma_{2k+1}(t_i)$, for $i = 1, \dots, \ell$, and its distance to any other $\gamma_{2k+1}(t)$, $t \in \mathbb{S}^1$, is at least r . Hence, q lies in the intersection $\bigcap_{i=1}^\ell \partial F_{2k+1}(t_i)$. \square

7.4 The modulus of discontinuity of ψ_{2k+1} is minimal

The theorem below is obtained as consequence of current knowledge of the structure of the Barvinok-Novik \mathcal{B}_{2k} and the relationship between convex hulls and Voronoi tilings induced by points on spheres. This theorem can be interpreted as emphasizing one particular aspect in which the TMC is optimal.

Theorem 9. $\text{disc}(\psi_{2k+1}) = \text{disc}(\psi_{2k}) = \delta_k = \frac{2k\pi}{2k+1}$.

Proof of Theorem 9. By Theorem 2 and Proposition 4.1, it suffices to prove that $\text{disc}(\psi_{2k+1}) \leq \delta_k$. To this end, we are going to invoke Corollary 5.1 which states that

$$\text{disc}(\psi_{2k+1}) = \min\{t \in [0, \pi] \mid \partial F_{2k+1}(0) \cap \partial F_{2k+1}(t) \neq \emptyset\}.$$

Assume that $t \in [0, \pi]$ is such that $\partial F_{2k+1}(0) \cap \partial F_{2k+1}(t) \neq \emptyset$. By Corollary 7.2, $d_1(0, t) \leq \delta_k$. Thus, $\text{disc}(\psi_{2k+1}) \leq \delta_k$. \square

7.5 Additional results stemming from Proposition 7.2

8 Results for the case \mathbb{S}^m versus \mathbb{S}^n

9 Historical account and connections

Our project about the precise determination of the Gromov-Hausdorff distance between spheres was started around 2003 in the context of the PhD thesis of the first author (FM). Part of the thesis was devoted to applications of the GH distance in shape matching/comparison

applications. This required developing some code for computing/estimating the distance. However, the code that was developed was not provably correct, in the sense that it used a number of heuristics in order to estimate the value of the distance. One observation made back then was that if the actual values of GH distance on a collection of canonical shapes were determined via theoretical methods then one would be able to assess the quality of said software by comparing the theoretically predicted value with the value produced by the software. It was eventually established that the computational problem posed by the GH distance is NP hard in the PhD work of Schmiedl [Sch17].

In 2007, during an Applied Topology seminar at Stanford, Tigran Ishkhanov suggested to FM the possibility of invoking the Borsuk-Ulam theorem in the context of the problem of computing the GH distance between spheres. This did not seem immediately useful as the standard version of the BU theorem is only applicable to continuous functions which are not, a priori, present in the definition of the GH distance. During the same seminar meeting, Gunnar Carlsson suggested using the stability of persistent homology for obtaining efficient lower bounds for the GH distance between spheres. This thread was explored in the research leading to [LMO24] and [MZ23]. The former approach would be revisited later (see below).

Around 2013/2014 this problem was energetically discussed in group meetings at OSU in which the second author (ZS) participated. Circa 2014/2015 ZS first constructed and experimentally tested the correspondences R_{γ_n} between \mathbb{S}^1 and \mathbb{S}^n for $n = 2, 3, 4, 5$. ZS found the shape of such curves through painstaking trial and error.⁹

Soon after that, FM tested these correspondences and constructed and tested the correspondence from Section 4.2.2 (between \mathbb{S}^1 and \mathbb{S}^2) as way of obtaining a correspondence which was somehow simpler than R_{γ_2} . This was then generalized to those correspondences described in Section 4.2.4 for spheres \mathbb{S}^m and \mathbb{S}^n of different dimension.

In the next few years the following took place:

- FM and ZS continued to experimentally test the correspondences R_{γ_n} while they also
- attempted to theoretically determine the distortion of these correspondences.
- Versions of these EPC correspondences applicable to spheres \mathbb{S}^m and \mathbb{S}^n of different dimension were also developed and tested extensively.
- Around 2015 Sunhyuk Lim (SL) became interested in the project and came on board to help develop the ideas that would eventually become [LMS23] and also those that led to the related project [LMO24].
- At some point in 2014/2015 they found a cartoonization of R_{γ_2} for which we were able to precisely determine its distortion. This cartoonization is explained in detail in [LMS21, Appendix D].
- Neither ZS or FM were aware of the connection between the correspondences R_{γ_n} and the TMC or the Barvinok-Novik polytope. In early 2017 Henry Adams visited OSU and, in the course of a conversation, ZS and FM shared with him that they

⁹Aided by classical multidimensional scaling methods in order to visualize the progressively better correspondences he obtained.

were working on the problem of determining the GH distance between spheres and described the TMC-EPC. During that conversation, Henry shared with FM and ZS that he had been learning about the Barvinok-Novik polytope and that he recognized that the curve they had been contemplating was known as the (symmetric) TMC in the literature about polytopes. Henry encouraged FM and ZS to look into that connection. Henry’s study of the TMC and the BN polytope eventually led to his joint work with Johnathan Bush and Florian Frick [ABF20, ABF23]. In a rather precise sense, ideas from both [ABF20] and [LMS23] were eventually combined in order to obtain the results in [ABC+22].

- One of the difficulties encountered when trying to determine the precise value of the distortion of R_{γ_n} and in establishing that it is optimal was the lack of knowledge about tight lower bounds for GH between spheres. The idea that was explored initially was to use the GH stability of persistent homology of Vietoris-Rips complexes to help in this regard. This led to [LMO24] and [MZ23] but did not end up giving tight lower bounds; see the discussion in [LMO24, Section 9.3.2] and [LMS23, Remark 1.13].
- At some point in 2019/2020 the authors of [LMS23] explored the idea of establishing suitable versions of the Borsuk-Ulam theorem to quantitatively obstruct the existence of low distortion correspondences between spheres of different dimension. This was FM’s interpretation of a suggestion made by Tigran Ishkhanov around 2007 (it took several years to eventually come around to this possibility which turned out to be very fruitful). In the summer of 2020, while reading [MBZ03] we found a mention of a version of the Borsuk-Ulam theorem applicable to discontinuous functions due to Dubins and Schwarz [DS81]. After some massaging (via the so called ‘helmet trick’ [LMS23, Lemma 5.7]) they were able to invoke this theorem in order to conclude that, for $n > m$, $d_{\text{GH}}(\mathbb{S}^n, \mathbb{S}^m) \geq \frac{1}{2}\zeta_m$ where $\zeta_m := \arccos\left(\frac{-1}{m+1}\right)$.
- When $m = 1$ and $n = 2, 3$, they experimentally determined that this lower bound, $\frac{\pi}{3}$, was matched by the distortions of R_{γ_2} and R_{γ_3} yet they were not able to prove this mathematically. This led to developing the correspondences used in [LMS23, Proposition 1.16 and 1.18] and in [LMS21, Appendix D] (for $n = 2, 3$) through the process of “cartoonization” mentioned earlier, which were substantially easier to analyze. A first version of [LMS23] was completed in 2021 [LMS21].
- In 2020/2021 Henry noticed a similarity between the table in [LMS23, Figure 2] and the table on [Bus19, page 11] and [Bus21, page 80] which made him suspect the existence of a quantitative connection between [LMS23] and [ABF20]. See [ABC+22, Question 8.12].
- From 2021 to 2022 a Polymath style group was formed with participants from Colorado State University, Carnegie Mellon, Ohio State and the Freie Universitet in Berlin. Many developments that combined ideas related to different threads came out of that project. See [ABC+22].
- One particular result obtained in the course of the Polymath activity was the lower bound given in Theorem 1, namely $d_{\text{GH}}(\mathbb{S}^1, \mathbb{S}^{2n}) \geq \frac{\pi n}{2n+1}$ and $d_{\text{GH}}(\mathbb{S}^1, \mathbb{S}^{2n+1}) \geq \frac{\pi n}{2n+1}$, for

arbitrary $n \geq 1$. This improved upon the lower bound $d_{\text{GH}}(\mathbb{S}^1, \mathbb{S}^n) \geq \frac{\pi}{3}$ for arbitrary n arising from [LMS23]. Henry conjectured these inequalities were in fact equalities. By providing a clear, explicit, lower bound, this has a direct impact on the analysis of the correspondences R_{γ_n} : to prove they are optimal, one just needs to prove their distortion is bounded above by twice the lower bound.

- Prompted by Henry, starting early in the course of the Polymath, FM described the general EPC idea as well as the TMC-EPC version to all the participants. During one of the subsequent meetings, Johnathan Bush described having experimented with the case of R_{γ_7} and obtaining results that matched the lower bound $\frac{7\pi}{15}$ predicted by Theorem 1. In subsequent meetings, FM described cartoonizations of the TMC-EPC via geodesic segments, generalizations, as well as some germs of the results presented in this writeup.
- In July 2022, in the context of the Polymath, Amzi Jeffs and Michael Harrison started exploring a construction of correspondences between \mathbb{S}^m and \mathbb{S}^n arising through first identifying suitable finite centrally symmetric point sets on each sphere in order to then partition spheres into Voronoi cells. These correspondences are structurally related to and inspired by the ones described in [LMS23] and especially to those in [LMS21, Appendix D]. By carefully designing these points sets, Amzi and Michael managed to prove they were optimal for all $(n, m) = (1, 2k)$, $k \geq 1$. This led to the results in [HJ23] containing the first complete description of a family of optimal correspondences between \mathbb{S}^1 and *all* even dimensional spheres.
- More or less simultaneously, in November 2022, Amzi and Michael started thinking of possible ways of constructing optimal correspondences between \mathbb{S}^1 and all odd dimensional spheres. For this they explored constructions inspired by the TMC-EPC (especially cartoonizations via piecewise geodesic curves). In April 2023 they reported having been able to prove that the correspondences they constructed were optimal. An upcoming update to [HJ23] will describe this construction and establish its optimality. Therefore, these results in combination with the ones described in the previous bullet point, provide the first complete answer to Question 1 for the value $m = 1$.

References

- [ABC⁺22] Henry Adams, Johnathan Bush, Nate Clause, Florian Frick, Mario Gómez, Michael Harrison, R Amzi Jeffs, Evgeniya Lagoda, Sunhyuk Lim, Facundo Mémoli, et al. Gromov-Hausdorff distances, Borsuk-Ulam theorems, and Vietoris-Rips complexes. *arXiv preprint arXiv:2301.00246*, 2022.
- [ABF20] Henry Adams, Johnathan Bush, and Florian Frick. Metric thickenings, Borsuk-Ulam theorems, and orbitopes. *Mathematika*, 66(1):79–102, 2020.
- [ABF23] Henry Adams, Johnathan Bush, and Florian Frick. The topology of projective codes and the distribution of zeros of odd maps. *Michigan Mathematical Journal*, 1(1):1–22, 2023.

- [Bar17] Alexander Barvinok. The beauty and the mystery of the symmetric moment curve. *Discrete Geometry and Convexity in Honour of Imre Bárány*, page 19, 2017.
- [BKS24] Paul Breiding, Kathlen Kohn, and Bernd Sturmfelds. *Metric algebraic geometry*, volume Oberwolfach Seminar 53. Birkhäuser, 2024.
- [BLN13] Alexander Barvinok, Seung Jin Lee, and Isabella Novik. Neighborliness of the symmetric moment curve. *Mathematika*, 59(1):223–249, 2013.
- [BN08] Alexander Barvinok and Isabella Novik. A centrally symmetric version of the cyclic polytope. *Discrete & Computational Geometry*, 39(1-3):76–99, 2008.
- [Bro79a] Kevin Q Brown. *Geometric transforms for fast geometric algorithms*. PhD thesis, Carnegie-Mellon University Pittsburgh, PA, 1979.
- [Bro79b] Kevin Q Brown. Voronoi diagrams from convex hulls. *Information processing letters*, 9(5):223–228, 1979.
- [Bus19] Johnathan Bush. Dissertation proposal: Simplicial metric thickenings of spheres. https://people.clas.ufl.edu/henry-adams/files/JohnBush_ThesisProposal2019.pdf, 2019.
- [Bus21] Johnathan E Bush. *Topological, geometric, and combinatorial aspects of metric thickenings*. PhD thesis, Colorado State University, 2021.
- [DS81] Lester Dubins and Gideon Schwarz. Equidiscontinuity of Borsuk-Ulam functions. *Pacific Journal of Mathematics*, 95(1):51–59, 1981.
- [FIN13] Orizon Pereira Ferreira, Alfredo N Iusem, and Sándor Zoltán Németh. Projections onto convex sets on the sphere. *Journal of Global Optimization*, 57(3):663–676, 2013.
- [For17] Steven Fortune. Voronoi diagrams and delaunay triangulations. In *Handbook of discrete and computational geometry*, pages 705–721. Chapman and Hall/CRC, 2017.
- [HJ23] Michael Harrison and R Amzi Jeffs. Quantitative upper bounds on the Gromov-Hausdorff distance between spheres. *arXiv preprint arXiv:2309.11237*, 2023.
- [LMO24] Sunhyuk Lim, Facundo Memoli, and Osman Berat Okutan. Vietoris-Rips persistent homology, injective metric spaces, and the filling radius. *Algebraic and Geometric Topology*, 24, 2024.
- [LMS21] Sunhyuk Lim, Facundo Mémoli, and Zane Smith. The Gromov-Hausdorff distance between spheres. *arXiv preprint arXiv:2105.00611*, 2021.
- [LMS23] Sunhyuk Lim, Facundo Mémoli, and Zane Smith. The Gromov-Hausdorff distance between spheres. *Geometry & Topology*, 27(9):3733–3800, 2023.

- [MBZ03] Jiří Matoušek, Anders Björner, and Günter M Ziegler. *Using the Borsuk-Ulam theorem: lectures on topological methods in combinatorics and geometry*, volume 2003. Springer, 2003.
- [MS23] Facundo Mémoli and Zane Smith. EPCs for the Gromov-Hausdorff distance between spheres. <https://github.com/ndag/dgh-spheres>, 2023.
- [MZ23] Facundo Mémoli and Ling Zhou. Persistent homotopy groups of metric spaces. *Journal of Topology and Analysis (to appear)*, 2023.
- [Sch17] Felix Schmiedl. Computational aspects of the Gromov–Hausdorff distance and its application in non-rigid shape matching. *Discrete & Computational Geometry*, 57(4):854–880, 2017.
- [Sin13] Rainer Sinn. Algebraic boundaries of $so(2)$ $so(2)$ -orbitopes. *Discrete & Computational Geometry*, 50:219–235, 2013.
- [Smi90] Zeev Smilansky. Bi-cyclic 4-polytopes. *Israel Journal of Mathematics*, 70:82–92, 1990.
- [Vin11] Cynthia Vinzant. Edges of the Barvinok–Novik orbitope. *Discrete & Computational Geometry*, 46(3):479–487, 2011.